

Trust Region Masking for Long-Horizon LLM Reinforcement Learning

Yingru Li*, Jiacai Liu^{*,1}, Jiawei Xu^{*,2}, Yuxuan Tong, Ziniu Li²,
Qian Liu, and Baoxiang Wang²

¹*Fudan University*, ²*The Chinese University of Hong Kong, Shenzhen*

Abstract

Policy gradient methods for Large Language Models optimize a policy π_θ via a surrogate objective computed from samples of a rollout policy π_{roll} . However, modern LLM-RL pipelines suffer from unavoidable implementation divergences, such as backend discrepancies, Mixture-of-Experts routing discontinuities, and distributed training staleness. These factors cause an off-policy mismatch ($\pi_{\text{roll}} \neq \pi_\theta$), leading to approximation errors between the surrogate and the true objective. We demonstrate that classical trust region bounds on this error scale as $O(T^2)$ with sequence length T , rendering them vacuous for long-horizon tasks. To address this, we derive two new bounds: a *Pinsker-Marginal* bound scaling as $O(T^{3/2})$ and a *Mixed* bound scaling as $O(T)$. We further derive an *Adaptive* bound that strictly generalizes the Pinsker-Marginal bound by combining an importance-ratio decomposition of the error with an adaptive per-position application of Pinsker’s inequality on the future trajectory divergence; the minimum over all three bounds is tighter than any individual bound. Crucially, all bounds depend on $D_{\text{KL}}^{\text{tok},\text{max}}$, the maximum token-level KL divergence across the sequence. As a *sequence-level* term, the divergence cannot be controlled by previous token-independent methods like PPO clipping. We propose Trust Region Masking (TRM), which masks entire sequences that violate the trust region. TRM enables the first non-vacuous monotonic improvement guarantees and demonstrates empirical training stability for long-horizon LLM-RL.

1 Introduction

Reinforcement Learning (RL) has emerged as a cornerstone in training Large Language Models (LLMs) for complex tasks that demand extended reasoning, multi-step problem solving, and agentic behavior. As LLMs are deployed for long-horizon applications—ranging from mathematical reasoning [Zeng et al., 2025] and code generation [Liu et al., 2024b] to autonomous tool use [Yang et al., 2024]—sequence lengths have rapidly expanded from hundreds to thousands of tokens. While policy gradient methods [Williams, 1992, Sutton et al., 1999], particularly Proximal Policy Optimization (PPO) [Schulman et al., 2017], remain the standard for these tasks, their theoretical foundations are increasingly strained by these extended horizons.

Trust region methods [Kakade and Langford, 2002, Schulman et al., 2015] offer a principled framework for policy optimization by utilizing a surrogate objective, $L(\pi_\theta)$, computed via samples from a rollout policy π_{roll} . The central appeal of this framework is the *monotonic improvement guarantee*: provided the surrogate objective improves and the policy remains within a specific trust

*Equal contribution

region, the true objective $J(\pi_\theta)$ is guaranteed to increase. However, this guarantee is predicated on bounding the approximation error $|J(\pi_\theta) - J(\pi_{\text{roll}}) - L(\pi_\theta)|$, a quantity strictly dependent on the divergence between the rollout policy π_{roll} and the training policy π_θ .

In the context of modern LLM-RL systems, recent work demonstrates that off-policy mismatch ($\pi_{\text{roll}} \neq \pi_\theta$) is not merely an implementation snag but an inevitable consequence of trust-region methods [Liu et al., 2025, Yao et al., 2025]. This mismatch arises from three primary sources:

- **Backend Discrepancies:** Discrepancies between high-throughput inference engines (e.g., vLLM [Kwon et al., 2023], SGLang [Zheng et al., 2024]) and precise training frameworks (e.g., Megatron-LM [Shoeybi et al., 2019], PyTorch FSDP [Zhao et al., 2023]) result in differing logits despite identical weights.
- **MoE Routing Discontinuities:** In Mixture-of-Experts models [Shazeer et al., 2017, Liu et al., 2024a], minor numerical jitter can flip the expert selection, causing high-magnitude jumps in token probabilities that disrupt the smoothness assumptions of standard RL.
- **Distributed Staleness:** Asynchronous training pipelines [Espeholt et al., 2018, Nair et al., 2015] introduce latency between data generation and gradient updates, resulting in training occurring on π_θ while rollouts are generated by stale weights π_{roll} .

We also provide a more detailed analysis of these mismatch sources in Appendix A.

Given that $\pi_{\text{roll}} \neq \pi_\theta$ is inevitable, the magnitude of the approximation error becomes a critical concern. Crucially, classical error bounds [Kakade and Langford, 2002, Schulman et al., 2015] scale quadratically with sequence length ($O(T^2)$). For modern reasoning tasks where responses frequently exceed $T = 4096$ tokens, these bounds become theoretically vacuous. Even with a negligible per-token divergence of $D_{\text{KL}}^{\text{tok},\text{max}} = 10^{-4}$, the classical bound predicts an error of ≈ 1677 —a value far exceeding any plausible reward improvement. Consequently, existing theory provides *no guarantee* that optimization steps in long-horizon LLM-RL actually improve performance.

To address this gap, we make the following contributions:

1. **Tighter Error Bounds:** We derive two novel bounds on the approximation error that significantly tighten theoretical guarantees: the *Pinsker-Marginal Bound* ($O(T^{3/2})$) and the *Mixed Bound* ($O(T)$). We further derive an *Adaptive Bound* that strictly generalizes the Pinsker-Marginal bound by combining a trajectory-level importance-ratio decomposition with a per-position adaptive application of Pinsker’s inequality. The minimum over all three bounds is tighter than any individual bound (Section 4).
2. **Analysis of Token-Level Failure:** We demonstrate that because both bounds depend on $D_{\text{KL}}^{\text{tok},\text{max}}$ —the maximum token-level divergence across the sequence—this error is inherently a sequence-level quantity. Consequently, it cannot be effectively controlled by token-independent interventions such as standard PPO clipping or token masking (Section 5).
3. **Trust Region Masking (TRM):** We propose TRM to mask entire sequences violating the trust region. By ensuring $D_{\text{KL}}^{\text{tok},\text{max}} \leq \delta$ for all accepted data and empirically verifying this condition globally, TRM enables non-vacuous monotonic improvement guarantees for long-horizon LLM-RL (Section 6). We additionally propose a length-neutral variant (LN-TRM) that mitigates the systematic bias against longer sequences inherent in any sequence-level masking criterion (Section D). Finally, we present empirical evidence demonstrating the training stability of TRM (Section 7).

2 Related Work

RL has become the standard paradigm for training LLMs in complex tasks where outcomes can be objectively verified, including mathematical reasoning [Lightman et al., 2023, Zeng et al., 2025] and code generation [Gu, 2023, Liu et al., 2024b]. However, applying policy gradient methods to reasoning chains that exceed thousands of tokens introduces severe stability challenges. Trust region methods, originating from Conservative Policy Iteration (CPI) [Kakade and Langford, 2002], provide the theoretical bedrock for stable RL training. TRPO [Schulman et al., 2015] practically applied these concepts by enforcing a KL divergence constraint between the training and rollout policies, guaranteeing monotonic improvement under the assumption that the divergence is small. However, the theoretical bounds underpinning these methods scale poorly with horizon length T . The classical result bounds the approximation error by $O(T^2)$ in the finite-horizon setting [Achiam et al., 2017]. While acceptable for short-horizon control tasks ($T \approx 100$), these bounds become vacuous for modern LLMs where T frequently exceeds 4000 tokens. Our work bridges this gap by deriving tight, non-vacuous bounds specifically for autoregressive sequence generation.

The divergence between the rollout and the training policy is a critical challenge in distributed RL. Frameworks like IMPALA [Espeholt et al., 2018] and APPO [Schulman et al., 2017] introduce correction mechanisms to mitigate staleness in actor-learner architectures. In the context of LLMs, this mismatch is exacerbated by the bifurcation of inference and training stacks. Rollout generation often utilizes high-throughput engines like vLLM [Kwon et al., 2023] or SGLang [Zheng et al., 2024], which may employ optimizations not present in the training loop (e.g., Megatron-LM [Shoeybi et al., 2019]). Recent studies characterize this “implementation divergence” as a primary driver of RL training instability [Liu et al., 2025, Yao et al., 2025].

Standard PPO implementations in LLMs enforce trust regions via token-level clipping [Ziegler et al., 2019]. However, autoregressive generation is inherently sequential; a small probability shift at an early token can lead to a vastly different semantic sequence, a phenomenon related to “exposure bias” [Bengio et al., 2015]. Our proposed Trust Region Masking (TRM) addresses this by enforcing constraints at the sequence level, ensuring that the theoretical preconditions for monotonic improvement are met in practice.

3 Background and Problem Setup

3.1 Autoregressive Language Generation

We focus on autoregressive language generation tasks where a policy π_θ generates a response $y = (y_1, \dots, y_T)$ given a prompt x . Each token y_t is sampled from a fixed vocabulary \mathcal{V} according to:

$$y_t \sim \pi_\theta(\cdot \mid x, y_{<t}), \quad (1)$$

where $y_{<t} = (y_1, \dots, y_{t-1})$ represents the sequence of tokens generated prior to step t . The probability distribution for the full trajectory factorizes as:

$$P^{\pi_\theta}(y \mid x) = \prod_{t=1}^T \pi_\theta(y_t \mid x, y_{<t}). \quad (2)$$

We define the *context* at step t as $c_t = (x, y_{<t})$. The *context visitation distribution* induced by the policy π is given by:

$$d_t^\pi(c_t) = P(x) \prod_{s=1}^{t-1} \pi(y_s \mid x, y_{<s}). \quad (3)$$

This distribution represents the probability of reaching a specific context c_t when following policy π .

3.2 The Optimization Problem

Given a scalar reward function $R(x, y) \in [0, 1]$, our objective is to maximize the expected reward:

$$J(\pi_\theta) = \mathbb{E}_{x \sim P(x)} \mathbb{E}_{y \sim \pi_\theta(\cdot|x)} [R(x, y)]. \quad (4)$$

A fundamental challenge in this setting is the off-policy mismatch: we generate samples from a *rollout policy* π_{roll} , which generally differs from the *training policy* π_θ . This necessitates the use of importance sampling or surrogate objectives to estimate gradients for π_θ .

3.3 The Surrogate Objective

Following Kakade and Langford [2002] and Schulman et al. [2015], we utilize the surrogate objective:

$$L_{\pi_{\text{roll}}}(\pi_\theta) = \mathbb{E}_{\pi_{\text{roll}}} \left[A \cdot \sum_{t=1}^T \rho_t \right], \quad (5)$$

where $A = R(x, y) - b$ denotes the trajectory advantage (relative to a baseline b), and

$$\rho_t = \frac{\pi_\theta(y_t | c_t)}{\pi_{\text{roll}}(y_t | c_t)} \quad (6)$$

is the per-token importance ratio. A critical property of this surrogate is that its gradient matches the true gradient at the reference policy [Kakade and Langford, 2002]:

$$\nabla L_{\pi_{\text{roll}}}(\pi_\theta) \big|_{\pi_\theta = \pi_{\text{roll}}} = \nabla J(\pi_\theta) \big|_{\pi_\theta = \pi_{\text{roll}}}. \quad (7)$$

While L serves as a valid local approximation of J , the approximation error grows as the divergence between π_θ and π_{roll} increases.

Remark 3.1 (Surrogate equivalence). *The error analysis in Section 4 and Appendix C employs the equivalent surrogate $L'_{\pi_{\text{roll}}}(\pi_\theta) = \mathbb{E}_{\pi_{\text{roll}}} [R(x, y) \sum_{t=1}^T (\rho_t - 1)]$. Since $\mathbb{E}_{\pi_{\text{roll}}} [\sum_t (\rho_t - 1)]$ does not depend on π_θ at $\pi_\theta = \pi_{\text{roll}}$ (where it equals zero), any fixed baseline b contributes a term that vanishes at the reference and does not affect the error $J(\pi_\theta) - J(\pi_{\text{roll}}) - L(\pi_\theta)$ up to a π_θ -independent constant. All bounds derived in this work apply equally to both forms.*

3.4 Divergence Measures

To quantify the discrepancy between policies, we employ the following divergence measures.

Definition 3.2 (Token-level divergences). *For a given context $c_t = (x, y_{<t})$, we define the Total Variation (TV) distance and the Kullback-Leibler (KL) divergence as:*

$$D_{\text{TV}}^{\text{tok}}(c_t) := D_{\text{TV}}(\pi_\theta(\cdot|c_t) \parallel \pi_{\text{roll}}(\cdot|c_t)) = \frac{1}{2} \sum_v |\pi_\theta(v|c_t) - \pi_{\text{roll}}(v|c_t)|, \quad (8)$$

$$D_{\text{KL}}(c_t) := D_{\text{KL}}(\pi_{\text{roll}}(\cdot|c_t) \parallel \pi_\theta(\cdot|c_t)) = \sum_v \pi_{\text{roll}}(v|c_t) \log \frac{\pi_{\text{roll}}(v|c_t)}{\pi_\theta(v|c_t)}. \quad (9)$$

Consistent with TRPO [Schulman et al., 2015], we utilize the KL divergence from the rollout policy to the training policy, $D_{\text{KL}}(\pi_{\text{roll}} \parallel \pi_{\theta})$. This direction is preferred because (1) it aligns with the constraint formulation in TRPO, and (2) it is computationally tractable using stored rollout logits.

Building on these token-level definitions, we define the corresponding sequence-level metrics:

Definition 3.3 (Maximum and sequence-level divergences).

$$D_{\text{TV}}^{\text{tok},\text{max}} := \max_{t,c_t} D_{\text{TV}}^{\text{tok}}(c_t), \quad (10)$$

$$D_{\text{KL}}^{\text{tok},\text{max}} := \max_{t,c_t} D_{\text{KL}}(c_t), \quad (11)$$

$$D_{\text{KL}}^{\text{seq}} := D_{\text{KL}}(P^{\pi_{\text{roll}}}(\cdot|x) \parallel P^{\pi_{\theta}}(\cdot|x)) = \sum_{t=1}^T \mathbb{E}_{c_t \sim d_t^{\pi_{\text{roll}}}} [D_{\text{KL}}(c_t)]. \quad (12)$$

We also define the *expected per-position TV divergence* along the rollout distribution:

$$\bar{D}_t := \mathbb{E}_{c_t \sim d_t^{\pi_{\text{roll}}}} [D_{\text{TV}}^{\text{tok}}(c_t)], \quad (13)$$

which plays a central role in data-dependent bounds (Section 4.4).

The relationship between the sequence-level KL and the token-level KL is governed by the chain rule. We formally state and prove this property below.

Lemma 3.4 (KL Chain Rule). *For any time step t , the divergence between context distributions decomposes as:*

$$D_{\text{KL}}(d_t^{\pi_{\text{roll}}} \parallel d_t^{\pi_{\theta}}) = \sum_{s=1}^{t-1} \mathbb{E}_{c_s \sim d_s^{\pi_{\text{roll}}}} [D_{\text{KL}}(c_s)]. \quad (14)$$

Proof. The joint trajectory distribution factorizes as $P^{\pi}(x, y_{<t}) = P(x) \prod_{s=1}^{t-1} \pi(y_s|c_s)$. The KL divergence is:

$$D_{\text{KL}}(d_t^{\pi_{\text{roll}}} \parallel d_t^{\pi_{\theta}}) = \mathbb{E}_{d_t^{\pi_{\text{roll}}}} \left[\sum_{s=1}^{t-1} \log \frac{\pi_{\text{roll}}(y_s|c_s)}{\pi_{\theta}(y_s|c_s)} \right] = \sum_{s=1}^{t-1} \mathbb{E}_{c_s \sim d_s^{\pi_{\text{roll}}}} [D_{\text{KL}}(c_s)]. \quad (15)$$

□

Note that the definition of $D_{\text{KL}}^{\text{seq}}$ in Eq. (12) corresponds to the special case considering the full sequence.

Finally, we recall Pinsker's inequality [Pinsker, 1964], which bounds the Total Variation by the KL divergence:

$$(D_{\text{TV}}^{\text{tok}})^2 \leq \frac{1}{2} D_{\text{KL}}. \quad (16)$$

Since the Total Variation distance is symmetric, Pinsker's inequality applies regardless of the KL direction. We use $D_{\text{KL}}(\pi_{\text{roll}} \parallel \pi_{\theta})$ as our primary measure of divergence throughout this work. Combined with the universal bound $D_{\text{TV}}^{\text{tok}} \leq 1$, this yields:

$$D_{\text{TV}}^{\text{tok}} \leq \min \left(1, \sqrt{\frac{D_{\text{KL}}}{2}} \right). \quad (17)$$

4 Theoretical Analysis

We develop tighter error bounds for the surrogate objective. We firstly define the approximation error as:

$$\text{Error}(\pi_\theta) := J(\pi_\theta) - J(\pi_{\text{roll}}) - L(\pi_\theta). \quad (18)$$

This quantity measures the discrepancy between the true objective improvement and the surrogate improvement. Bounding $|\text{Error}|$ is sufficient to guarantee that maximizing L leads to a monotonic improvement in J .

This error can be decomposed into a sum over timesteps using the Performance Difference Identity [Kakade and Langford, 2002]. Let the per-step advantage be $A_t^{\pi_{\text{roll}}}(c, y_t) := \mathbb{E}_{\pi_{\text{roll}}}[R | c, y_t] - \mathbb{E}_{\pi_{\text{roll}}}[R | c]$, and define the expected advantage as $g_t(c_t) := \mathbb{E}_{y_t \sim \pi_\theta}[A_t^{\pi_{\text{roll}}}(c_t, y_t)]$. The error is then given by:

$$\text{Error} = \sum_{t=1}^T \left(\mathbb{E}_{c_t \sim d_t^{\pi_\theta}}[g_t(c_t)] - \mathbb{E}_{c_t \sim d_t^{\pi_{\text{roll}}}}[g_t(c_t)] \right). \quad (19)$$

Intuitively, the error arises from evaluating the expected advantage g_t under the mismatching context distribution $d_t^{\pi_{\text{roll}}}$ rather than the true distribution $d_t^{\pi_\theta}$.

Our analysis relies on the following fundamental lemmas involving the advantage bound and context shift. We derive them formally below.

Lemma 4.1 (Martingale Property). *For any context c_t , the expected advantage under the rollout policy is zero: $\mathbb{E}_{y_t \sim \pi_{\text{roll}}(\cdot | c_t)}[A_t(c_t, y_t)] = 0$.*

Proof. By definition, $V(c_t) = \mathbb{E}_{y_t \sim \pi_{\text{roll}}}[Q(c_t, y_t)]$ and $A_t = Q - V$. Thus, $\mathbb{E}_{\pi_{\text{roll}}}[A_t] = \mathbb{E}_{\pi_{\text{roll}}}[Q - V] = V - V = 0$. \square

Lemma 4.2 (Advantage Bound). *For rewards $R \in [0, 1]$, the expected advantage shift is bounded by:*

$$|g_t(c_t)| \leq 2D_{\text{TV}}^{\text{tok}}(c_t) \leq 2 \min\left(1, \sqrt{\frac{D_{\text{KL}}(c_t)}{2}}\right). \quad (20)$$

In particular, $|g_t(c_t)| \leq 2$ always, and $\|g_t\|_\infty \leq 2 \min\left(1, \sqrt{D_{\text{KL}}^{\text{max}}/2}\right)$.

Proof. Using the Martingale Property (Lemma 4.1), we can rewrite g_t :

$$g_t(c_t) = \mathbb{E}_{\pi_\theta}[A_t] - \underbrace{\mathbb{E}_{\pi_{\text{roll}}}[A_t]}_{=0} = \sum_{y_t} (\pi_\theta(y_t | c_t) - \pi_{\text{roll}}(y_t | c_t)) \cdot A_t(c_t, y_t). \quad (21)$$

Since rewards are in $[0, 1]$, we have $|A_t| \leq 1$ (because $A_t = \mathbb{E}[R | c_t, y_t] - \mathbb{E}[R | c_t]$ and both conditional expectations lie in $[0, 1]$). Applying Hölder's inequality:

$$|g_t(c_t)| \leq \sum_{y_t} |\pi_\theta(y_t | c_t) - \pi_{\text{roll}}(y_t | c_t)| \cdot 1 = 2D_{\text{TV}}^{\text{tok}}(c_t). \quad (22)$$

Since $D_{\text{TV}}^{\text{tok}}(c_t) \leq 1$ for any pair of distributions, and by Pinsker's inequality $D_{\text{TV}}^{\text{tok}}(c_t) \leq \sqrt{D_{\text{KL}}(c_t)/2}$, the combined bound in Eq. (20) follows. \square

Lemma 4.3 (Context Shift). *The context distribution shift satisfies:*

$$\|d_t^{\pi_\theta} - d_t^{\pi_{\text{roll}}}\|_{\text{TV}} \leq \min\left(1, (t-1) \cdot D_{\text{TV}}^{\text{tok,max}}\right). \quad (23)$$

Moreover, by applying Pinsker's inequality to the marginal KL:

$$\|d_t^{\pi_\theta} - d_t^{\pi_{\text{roll}}}\|_{\text{TV}} \leq \min\left(1, \sqrt{\frac{(t-1) \cdot D_{\text{KL}}^{\text{tok,max}}}{2}}\right). \quad (24)$$

Proof. **Coupling bound:** We proceed by induction. **Base case** ($t = 1$): $d_1^{\pi_\theta} = d_1^{\pi_{\text{roll}}} = P(x)$, so the TV distance is 0. **Inductive step:** Using the coupling bound for product distributions:

$$\begin{aligned} \|d_{t+1}^{\pi_\theta} - d_{t+1}^{\pi_{\text{roll}}}\|_{\text{TV}} &\leq \|d_t^{\pi_\theta} - d_t^{\pi_{\text{roll}}}\|_{\text{TV}} + D_{\text{TV}}^{\text{tok,max}} \\ &\leq (t-1)D_{\text{TV}}^{\text{tok,max}} + D_{\text{TV}}^{\text{tok,max}} \\ &= t \cdot D_{\text{TV}}^{\text{tok,max}}. \end{aligned} \quad (25)$$

Since $\|d_t^{\pi_\theta} - d_t^{\pi_{\text{roll}}}\|_{\text{TV}} \leq 1$ for any pair of distributions, the capped bound Eq. (23) follows.

Pinsker bound: By the KL chain rule (Lemma 3.4):

$$D_{\text{KL}}(d_t^{\pi_{\text{roll}}} \parallel d_t^{\pi_\theta}) = \sum_{s=1}^{t-1} \mathbb{E}_{c_s \sim d_s^{\pi_{\text{roll}}}} [D_{\text{KL}}(c_s)] \leq (t-1) \cdot D_{\text{KL}}^{\text{tok,max}}. \quad (26)$$

Applying Pinsker's inequality $D_{\text{TV}} \leq \sqrt{D_{\text{KL}}/2}$ and capping at 1 yields Eq. (24). \square

4.1 The Failure of Classical Bounds

The classical TRPO bound is derived by combining these lemmas via the inequality $|\mathbb{E}_P[f] - \mathbb{E}_Q[f]| \leq 2\|f\|_\infty \cdot D_{\text{TV}}(P, Q)$. Using $\|g_t\|_\infty \leq 2D_{\text{TV}}^{\text{tok,max}}$ and $D_{\text{TV}}(d_t^{\pi_\theta}, d_t^{\pi_{\text{roll}}}) \leq (t-1)D_{\text{TV}}^{\text{tok,max}}$ without the caps, this yields:

$$|\text{Error}| \leq 4(D_{\text{TV}}^{\text{tok,max}})^2 \sum_{t=1}^T (t-1) = 2T(T-1)(D_{\text{TV}}^{\text{tok,max}})^2 \leq T(T-1) \cdot D_{\text{KL}}^{\text{tok,max}}. \quad (27)$$

This bound scales as $O(T^2)$. For a typical reasoning task with sequence length $T = 4096$ and a divergence of $D_{\text{KL}}^{\text{tok,max}} = 10^{-4}$, the bound yields $|\text{Error}| \leq 1677$. Since the maximum possible reward is 1, a bound of 1677 is *vacuous*, offering no theoretical guarantee of improvement.

We are now ready to introduce two tighter bounds that significantly reduce this scaling.

4.2 The Pinsker-Marginal Bound

Our key insight is to apply Pinsker's inequality [Pinsker, 1964, Cover, 1999] to the *marginal* KL divergence rather than summing the per-step TV distances.

Theorem 4.4 (Pinsker-Marginal Bound). *The approximation error is bounded by:*

$$|\text{Error}| \leq 4 \min\left(1, \sqrt{\frac{D_{\text{KL}}^{\text{tok,max}}}{2}}\right) \sum_{t=1}^T \min\left(1, \sqrt{\frac{(t-1) \cdot D_{\text{KL}}^{\text{tok,max}}}{2}}\right). \quad (28)$$

In the small-divergence regime where $D_{\text{KL}}^{\text{tok,max}} \leq 2/T$, all caps are inactive and this simplifies to:

$$|\text{Error}| \leq \frac{4}{3} T^{3/2} \cdot D_{\text{KL}}^{\text{tok,max}}. \quad (29)$$

Proof. From the context-shift decomposition (Eq. (19)) and the inequality $|\mathbb{E}_P[f] - \mathbb{E}_Q[f]| \leq 2\|f\|_\infty \cdot D_{\text{TV}}(P, Q)$:

$$|\text{Error}| \leq \sum_{t=1}^T 2\|g_t\|_\infty \cdot \|d_t^{\pi_\theta} - d_t^{\pi_{\text{roll}}}\|_{\text{TV}}. \quad (30)$$

Advantage term. By Lemma 4.2:

$$\|g_t\|_\infty \leq 2D_{\text{TV}}^{\text{tok,max}} \leq 2 \min\left(1, \sqrt{\frac{D_{\text{KL}}^{\text{tok,max}}}{2}}\right). \quad (31)$$

The first inequality is the Advantage Bound; the second applies Pinsker to $D_{\text{TV}}^{\text{tok,max}}$ and caps at the natural upper bound $D_{\text{TV}}^{\text{tok,max}} \leq 1$.

Context shift term. By Eq. (24) in Lemma 4.3:

$$\|d_t^{\pi_\theta} - d_t^{\pi_{\text{roll}}}\|_{\text{TV}} \leq \min\left(1, \sqrt{\frac{(t-1) \cdot D_{\text{KL}}^{\text{tok,max}}}{2}}\right). \quad (32)$$

Substituting Eq. (31) and Eq. (32) into Eq. (30) yields the full bound Eq. (28).

Small-divergence simplification. When $D_{\text{KL}}^{\text{tok,max}} \leq 2/T$, we have $(t-1)D_{\text{KL}}^{\text{tok,max}}/2 \leq (T-1)D_{\text{KL}}^{\text{tok,max}}/2 < 1$ for all $t \leq T$, and $D_{\text{KL}}^{\text{tok,max}}/2 < 1/T < 1$. Thus all $\min(\cdot)$ caps are inactive, and:

$$|\text{Error}| \leq 4 \cdot \sqrt{\frac{D_{\text{KL}}^{\text{tok,max}}}{2}} \cdot \sum_{t=1}^T \sqrt{\frac{(t-1)D_{\text{KL}}^{\text{tok,max}}}{2}} = 4 \cdot \frac{D_{\text{KL}}^{\text{tok,max}}}{2} \sum_{k=0}^{T-1} \sqrt{k}. \quad (33)$$

Using $\sum_{k=0}^{T-1} \sqrt{k} \leq \int_0^T \sqrt{x} dx = \frac{2}{3}T^{3/2}$:

$$|\text{Error}| \leq 2D_{\text{KL}}^{\text{tok,max}} \cdot \frac{2}{3}T^{3/2} = \frac{4}{3}T^{3/2} \cdot D_{\text{KL}}^{\text{tok,max}}. \quad (34)$$

□

For $T = 4096$ and $D_{\text{KL}}^{\text{tok,max}} = 10^{-4}$, we have $2/T \approx 4.9 \times 10^{-4} > 10^{-4}$, confirming the small-divergence regime. The simplified bound yields $|\text{Error}| \leq 35.0$, a $48\times$ improvement over the classical result.

4.3 The Mixed Bound

We can also bound the context-shift TV uniformly using the full sequence-level KL divergence.

Theorem 4.5 (Mixed Bound). *The approximation error is bounded by:*

$$|\text{Error}| \leq 4T \cdot \min\left(1, \sqrt{\frac{D_{\text{KL}}^{\text{tok,max}}}{2}}\right) \cdot \min\left(1, \sqrt{\frac{D_{\text{KL}}^{\text{seq}}}{2}}\right). \quad (35)$$

When both $D_{\text{KL}}^{\text{tok,max}} \leq 2$ and $D_{\text{KL}}^{\text{seq}} \leq 2$ (so both caps are inactive), this simplifies to:

$$|\text{Error}| \leq 2T \cdot \sqrt{D_{\text{KL}}^{\text{tok,max}} \cdot D_{\text{KL}}^{\text{seq}}}. \quad (36)$$

Proof. The marginal KL at any step t is bounded by the full sequence KL:

$$D_{\text{KL}}(d_t^{\pi_{\text{roll}}} \parallel d_t^{\pi_{\theta}}) = \sum_{s=1}^{t-1} \mathbb{E}[D_{\text{KL}}(c_s)] \leq \sum_{s=1}^T \mathbb{E}[D_{\text{KL}}(c_s)] = D_{\text{KL}}^{\text{seq}}. \quad (37)$$

The inequality holds because all summands are non-negative. Applying Pinsker's inequality and capping at 1:

$$\|d_t^{\pi_{\theta}} - d_t^{\pi_{\text{roll}}}\|_{\text{TV}} \leq \min\left(1, \sqrt{\frac{D_{\text{KL}}^{\text{seq}}}{2}}\right). \quad (38)$$

This bound is uniform in t , so summing over T steps and using the capped advantage bound (31):

$$\begin{aligned} |\text{Error}| &\leq \sum_{t=1}^T 2 \cdot 2 \min\left(1, \sqrt{\frac{D_{\text{KL}}^{\text{tok,max}}}{2}}\right) \cdot \min\left(1, \sqrt{\frac{D_{\text{KL}}^{\text{seq}}}{2}}\right) \\ &= 4T \cdot \min\left(1, \sqrt{\frac{D_{\text{KL}}^{\text{tok,max}}}{2}}\right) \cdot \min\left(1, \sqrt{\frac{D_{\text{KL}}^{\text{seq}}}{2}}\right). \end{aligned} \quad (39)$$

When both caps are inactive: $4T \cdot \sqrt{D_{\text{KL}}^{\text{tok,max}}/2} \cdot \sqrt{D_{\text{KL}}^{\text{seq}}/2} = 2T \sqrt{D_{\text{KL}}^{\text{tok,max}} \cdot D_{\text{KL}}^{\text{seq}}}$. \square

This bound is strictly tighter when the divergence is sparse (i.e., $D_{\text{KL}}^{\text{seq}}$ is small relative to $T \cdot D_{\text{KL}}^{\text{tok,max}}$). For $D_{\text{KL}}^{\text{seq}} = 0.01$, this yields $|\text{Error}| \leq 8.2$, a $200\times$ improvement over TRPO.

4.4 The Adaptive Bound via Importance-Ratio Decomposition

The Pinsker-Marginal and Mixed bounds both use the *context-shift decomposition* (Eq. (19)), which bounds the advantage term by its worst case ($\|g_t\|_{\infty} \leq 2D_{\text{TV}}^{\text{tok,max}}$) and then controls the context shift. This sacrifices information about the *actual* per-position divergence \bar{D}_t .

We now derive a strictly tighter bound using an alternative decomposition based on importance ratios, which preserves this per-position structure. The key idea is to decompose the error into a per-token “local deviation” factor and a “future-trajectory divergence” factor, then apply Pinsker’s inequality *adaptively* to the future factor at each position.

Theorem 4.6 (Adaptive Bound). *The approximation error satisfies:*

$$|\text{Error}| \leq 4 \sum_{t=1}^T \bar{D}_t \cdot \min\left(1, \sqrt{\frac{(T-t) D_{\text{KL}}^{\text{tok,max}}}{2}}\right), \quad (40)$$

where $\bar{D}_t = \mathbb{E}_{c_t \sim d_t^{\pi_{\text{roll}}}}[D_{\text{TV}}^{\text{tok}}(c_t)]$ is the expected per-position TV divergence. Note that

$$\bar{D}_t \leq \min(1, \sqrt{D_{\text{KL}}^{\text{tok,max}}/2})$$

always. This bound is strictly tighter than both the Pinsker-Marginal bound (Theorem 4.4) and the linear bound $4T \cdot D_{\text{TV}}^{\text{tok,max}}$ (recovered as a special case; see Remark 4.7).

The proof is given in Appendix C. The derivation proceeds via an importance-ratio decomposition of the error:

Step 1. Decompose the exact error identity $J(\pi_\theta) - J(\pi_{\text{roll}}) = L'(\pi_\theta) - \Delta$ where $\Delta = \mathbb{E}_{y \sim \pi_{\text{roll}}} [R(y) \sum_t (\rho_t - 1)(1 - \prod_{j > t} \rho_j)]$ (this is an algebraic identity, not an approximation).

Step 2. Apply the tower property to separate the per-token factor $|\rho_t - 1|$ from the future-trajectory factor $|1 - \prod_{j > t} \rho_j|$. Conditioned on c_{t+1} , the expected future factor equals

$$2D_{\text{TV}}(P^{\pi_{\text{roll}}}(\cdot | c_{t+1}) \| P^{\pi_\theta}(\cdot | c_{t+1})),$$

where $P^\pi(\cdot | c_{t+1})$ denotes the distribution over future trajectories (y_{t+1}, \dots, y_T) under policy π .

Step 3. Bound the future-trajectory TV adaptively at each position via:

$$D_{\text{TV}}(P^{\pi_{\text{roll}}}(\cdot | c_{t+1}) \| P^{\pi_\theta}(\cdot | c_{t+1})) \leq \min \left(1, \sqrt{\frac{(T-t) D_{\text{KL}}^{\text{tok,max}}}{2}} \right), \quad (41)$$

using either the trivial bound $D_{\text{TV}} \leq 1$ or Pinsker's inequality applied to the future conditional KL (which is $\leq (T-t) D_{\text{KL}}^{\text{tok,max}}$), whichever is smaller.

Step 4. Since the min holds for *every* realization of c_{t+1} , it can be pulled outside the outer expectation, yielding the bound with \bar{D}_t .

The result is tighter than the Pinsker-Marginal bound in two independent ways:

1. **Data-dependent advantage:** The factor \bar{D}_t (expected per-position TV) replaces $D_{\text{TV}}^{\text{tok,max}}$ (worst-case per-position TV). When divergence is non-uniform across positions—e.g., concentrated at a few tokens due to MoE routing flips— $\bar{D}_t \ll D_{\text{TV}}^{\text{tok,max}}$ at most positions.
2. **Adaptive future bounding:** The $\min(1, \cdot)$ caps the future-trajectory TV at 1 for positions near the end of the sequence (where $T-t$ is small), preventing the Pinsker estimate $\sqrt{(T-t) D_{\text{KL}}^{\text{tok,max}}}/2$ from exceeding the trivial bound. For positions near the beginning, it uses the tighter Pinsker estimate.

Remark 4.7 (Relationship to prior bounds). *Setting $\bar{D}_t = \min(1, \sqrt{D_{\text{KL}}^{\text{tok,max}}}/2)$ (the worst-case per-position TV via Pinsker) and noting the sum identity $\sum_t f(T-t) = \sum_t f(t-1)$, we see that the Adaptive bound with uniform worst-case divergence recovers exactly the full Pinsker-Marginal bound Eq. (28), including all $\min(1, \cdot)$ caps. Setting $\bar{D}_t = D_{\text{TV}}^{\text{tok,max}}$ and using only the $\min = 1$ branch recovers the linear bound $4T \cdot D_{\text{TV}}^{\text{tok,max}}$.¹ The Adaptive bound interpolates between these, always being at least as tight as either, and strictly tighter when both $\bar{D}_t < D_{\text{TV}}^{\text{tok,max}}$ at some positions and the crossover point $t^* = T - 2/D_{\text{KL}}^{\text{tok,max}}$ falls within $[1, T]$.*

4.5 Summary and Implications

We combine all results into a unified adaptive bound. Defining the minorizer $\mathcal{M}(\pi_\theta) := L(\pi_\theta) - |\text{Error}|_b$ with the bound error, monotonic improvement ($J(\pi_\theta) > J(\pi_{\text{roll}})$) is guaranteed if $\mathcal{M}(\pi_\theta) > 0$, where:

$$|\text{Error}|_b = \min \{B_{\text{PM}}, B_{\text{Mix}}, B_{\text{Adap}}\}, \quad (42)$$

¹This linear special case was independently noted by Qi et al. [2026].

with:

$$B_{\text{PM}} = 4 \min \left(1, \sqrt{\frac{D_{\text{KL}}^{\text{tok,max}}}{2}} \right) \sum_{t=1}^T \min \left(1, \sqrt{\frac{(t-1)D_{\text{KL}}^{\text{tok,max}}}{2}} \right), \quad (43)$$

$$B_{\text{Mix}} = 4T \cdot \min \left(1, \sqrt{\frac{D_{\text{KL}}^{\text{tok,max}}}{2}} \right) \cdot \min \left(1, \sqrt{\frac{D_{\text{KL}}^{\text{seq}}}{2}} \right), \quad (44)$$

$$B_{\text{Adap}} = 4 \sum_t \bar{D}_t \cdot \min \left(1, \sqrt{\frac{(T-t)D_{\text{KL}}^{\text{tok,max}}}{2}} \right). \quad (45)$$

Since each bound holds independently, the minimum is valid. The first two bounds are worst-case (depending only on $D_{\text{KL}}^{\text{tok,max}}$ and $D_{\text{KL}}^{\text{seq}}$), while the third is data-dependent (requiring the per-position divergences \bar{D}_t). In the small-divergence regime ($D_{\text{KL}}^{\text{tok,max}} \leq 2/T$, $D_{\text{KL}}^{\text{seq}} \leq 2$), the caps are inactive and the expressions simplify to $\frac{4}{3}T^{3/2}D_{\text{KL}}^{\text{tok,max}}$, $2T\sqrt{D_{\text{KL}}^{\text{tok,max}} \cdot D_{\text{KL}}^{\text{seq}}}$, and the adaptive sum, respectively.

Table 1: Comparison of error bounds across two regimes ($T = 4096$). **Small-divergence** ($D_{\text{KL}}^{\text{tok,max}} = 10^{-4}$, $D_{\text{KL}}^{\text{seq}} = 0.01$): the $\min(1, \cdot)$ caps do not bind. **Large-divergence** ($D_{\text{KL}}^{\text{tok,max}} = 1$, $D_{\text{KL}}^{\text{seq}} = 1$): the context-shift cap in the Pinsker-Marginal bound binds (marked \dagger); the advantage and mixed context caps remain inactive ($\sqrt{1/2} \approx 0.71 < 1$). Rows labelled “no cap” show what happens if the $\min(1, \cdot)$ is removed.

Bound	Scaling	Small div.		Large div. ($D_{\text{KL}}^{\text{tok,max}} = 1$)	
		$D_{\text{KL}}^{\text{tok,max}} = 10^{-4}$	no cap	with cap	with cap
Classical (TRPO)	$O(T^2)$		1,677		1.68×10^7
Linear	$O(T)$		115.9		11,585
Pinsker-Marginal	$O(T^{3/2})$		35.0	3.49×10^5	11,582 \dagger
Mixed	$O(T)$		8.2		8,192
Adaptive	\leq all above		$\leq 8.2^*$	—	$\leq 8,192^*$

\dagger The context-shift cap $\min(1, \sqrt{(t-1)D_{\text{KL}}^{\text{tok,max}}/2})$ saturates at 1 for 4,094 of 4,096 positions ($t \geq 3$), reducing the uncapped PM value by 30×. * Adaptive bound takes the minimum of all rows above (Mixed in both regimes).

Crucially, all bounds depend on $D_{\text{KL}}^{\text{tok,max}}$, the maximum token-level divergence. This confirms that the error is inherently a *sequence-level* quantity; controlling the average token KL is insufficient. We formalize the impossibility of removing this dependence in the following proposition.

Proposition 4.8. *There exists no function $f : \mathbb{R}^+ \rightarrow \mathbb{R}^+$ such that $D_{\text{KL}}^{\text{tok,max}} \leq f(D_{\text{KL}}^{\text{seq}})$ for all policy pairs.*

Proof. Consider a context c^* that occurs with probability ϵ under the rollout distribution $d_t^{\pi_{\text{roll}}}$. Let the divergence be concentrated solely at this context: $D_{\text{KL}}(c^*) = 1$ and $D_{\text{KL}}(c) = 0$ for all $c \neq c^*$.

Then, the maximum token divergence is $D_{\text{KL}}^{\text{tok,max}} = 1$ (constant, independent of ϵ). However, the sequence-level divergence is $D_{\text{KL}}^{\text{seq}} = \epsilon \cdot 1 + (1 - \epsilon) \cdot 0 = \epsilon$. As $\epsilon \rightarrow 0$, $D_{\text{KL}}^{\text{seq}} \rightarrow 0$ while $D_{\text{KL}}^{\text{tok,max}}$ remains 1. Thus, knowing only that $D_{\text{KL}}^{\text{seq}}$ is small provides no upper bound on $D_{\text{KL}}^{\text{tok,max}}$. \square

This result necessitates our approach: sequence-level masking based on the *maximum* token divergence is required because token-level operations cannot control the worst-case error that drives training collapse.

5 Why Token-Level Methods Fail

Our theoretical analysis establishes that the approximation error is strictly bounded by $D_{\text{KL}}^{\text{tok},\max}$ —a property of the *entire sequence*. In this section, we analyze why standard token-level interventions, such as PPO clipping or token masking, are mathematically insufficient to control this quantity, thereby failing to prevent optimization collapse in the presence of off-policy mismatch.

5.1 PPO Clipping and Gradient Leakage

PPO [Schulman et al., 2017] attempts to constrain updates via a clipped surrogate objective:

$$L^{\text{CLIP}}(\pi_\theta) = \mathbb{E} \left[\sum_{t=1}^T \min(\rho_t A_t, \text{clip}(\rho_t, 1-\epsilon, 1+\epsilon) A_t) \right]. \quad (46)$$

While effective for standard control tasks, this mechanism fails when faced with the severe logit discrepancies common in LLMs. The failure mode is structural: the clipping operator $\text{clip}(\cdot)$ is asymmetric. As detailed in Table 2, the mechanism provides safety when the policy attempts to increase the probability of a “good” action (Positive Advantage). However, it offers no protection against the penalization of “bad” actions (Negative Advantage) when the importance ratio ρ_t is erroneously high (e.g., $\rho_t \gg 1 + \epsilon$).

Table 2: PPO Clipping Analysis. When off-policy mismatch causes a spike in ρ_t (e.g., due to MoE routing jitter), negative advantages result in **unbounded** gradients.

Ratio ρ_t	Advantage A_t	Objective Value	Outcome
$> 1 + \epsilon$	> 0	$(1 + \epsilon)A_t$	Clipped (Safe)
$< 1 - \epsilon$	< 0	$(1 - \epsilon)A_t$	Clipped (Safe)
$> 1 + \epsilon$	< 0	$\rho_t A_t$	Unclipped (Unbounded)
$< 1 - \epsilon$	> 0	$\rho_t A_t$	Unclipped (Unbounded)

In standard RL, this behavior is intended to penalize actions that are much more likely under the training policy but yield poor returns. However, in the context of mismatch in LLMs (e.g., implementation divergence), a large ρ_t often represents numerical noise rather than a meaningful policy shift. Consequently, the optimizer receives a massive, erroneous gradient update that pushes the weights destructively, leading to the training collapse observed in practice.

5.2 The Insufficiency of Token Masking

A common heuristic to mitigate this is *token masking*: zeroing out the gradient contribution of specific tokens where $|\log \rho_t| > \delta$. The modified gradient becomes:

$$\nabla \approx \sum_{t=1}^T M_t \cdot \rho_t \nabla \log \pi_\theta(y_t | c_t) \cdot A, \quad (47)$$

where $M_t = 0$ if the divergence condition is met.

While this prevents immediate gradient explosion, it fails to satisfy the theoretical requirements for monotonic improvement. The error bounds derived in Section 4 depend on the divergence between the distributions π_{roll} and π_θ over the *entire trajectory*. Masking a specific token t in the gradient computation does not alter the fact that the rollout distribution π_{roll} has diverged from π_θ . The quantity $D_{\text{KL}}^{\text{tok},\text{max}}$ remains high, rendering the error bound vacuous. We formalize this limitation in the following proposition:

Proposition 5.1. *Token masking preserves vacuous bounds.* *Let $\mathcal{T}_{\text{mask}}$ be a token-level masking operator. The maximum token-level divergence of the underlying process remains unchanged:*

$$D_{\text{KL}}^{\text{tok},\text{max}}(\pi_\theta, \pi_{\text{roll}}) = D_{\text{KL}}^{\text{tok},\text{max}}(\mathcal{T}_{\text{mask}}(\pi_\theta), \pi_{\text{roll}}). \quad (48)$$

Consequently, token masking alters the optimization direction but fails to restore the validity of the monotonic improvement guarantee.

5.3 The Sequence-Level Imperative

Neither approach satisfies the theoretical requirements: standard PPO suffers from severe gradient leakage, while token masking prevents leakage but leaves $D_{\text{KL}}^{\text{tok},\text{max}}$ unchanged, so the error bound remains vacuous. The root cause is that the approximation error is cumulative and depends on the worst-case divergence in the sequence. If *any* token violates the trust region, the validity of the entire trajectory as an estimator for $J(\pi_\theta)$ is compromised. Therefore, relying on the tighter bounds derived in this work, we must exclude the *entire sequence* from the gradient computation, as proposed in Trust Region Masking (TRM).

6 Trust Region Masking

The theoretical analysis in Section 4 establishes that the approximation error is governed by $D_{\text{KL}}^{\text{tok},\text{max}}$ —a sequence-level quantity. Consequently, standard token-level interventions (such as PPO clipping) are insufficient to guarantee monotonic improvement. To address this, we propose **Trust Region Masking (TRM)**, which masks *entire sequences* that violate the trust region constraints.

6.1 The Masked Surrogate Objective

We define a binary sequence mask $M(x, y) = \mathbb{I}[(x, y) \in \text{Trust Region}]$ and the corresponding masked surrogate objective:

$$L_{\text{masked}}(\pi_\theta) = \mathbb{E}_{\pi_{\text{roll}}} \left[M(x, y) \cdot A(x, y) \cdot \sum_{t=1}^T \rho_t \right]. \quad (49)$$

The gradient is estimated using a batch of N samples:

$$\nabla L_{\text{masked}} \approx \frac{1}{N} \sum_{i=1}^N M_i \cdot A^{(i)} \cdot \sum_{t=1}^T \rho_t^{(i)} \nabla \log \pi_\theta(y_t^{(i)} | c_t^{(i)}). \quad (50)$$

Crucially, the normalization factor is the *total* batch size N , not the count of accepted sequences. This ensures that rejected sequences effectively contribute zero gradient, preserving the unbiased nature of the estimate over the valid trust region. This acts as a rejection sampling mechanism: we simply choose not to learn from trajectories where the off-policy divergence renders the gradient unreliable.

Algorithm 1 Trust Region Masking (TRM)

Require: Threshold δ ; Batch $\mathcal{D} = \{(x^{(i)}, y^{(i)})\}_{i=1}^N$; Stored π_{roll} logits

- 1: **Forward Pass:** Compute logits for π_θ on all data $(x, y) \in \mathcal{D}$
- 2: **for** each sequence $i \in \{1, \dots, N\}$ **do**
- 3: Compute per-token KL: $D_{\text{KL}}(c_t^{(i)}) = D_{\text{KL}}(\pi_{\text{roll}}(\cdot|c_t^{(i)}) \parallel \pi_\theta(\cdot|c_t^{(i)}))$
- 4: Compute mask: $M_i \leftarrow \mathbb{I}[\max_t D_{\text{KL}}(c_t^{(i)}) \leq \delta]$
- 5: **end for**
- 6: **Backward Pass:** Compute ∇L_{masked} using only samples where $M_i = 1$
- 7: **Update:** $\theta \leftarrow \theta + \alpha \cdot \nabla L_{\text{masked}}$

6.2 Implementation and Divergence Estimation

Exact KL Computation. Following TRPO [Schulman et al., 2015], we utilize the forward KL divergence $D_{\text{KL}}(\pi_{\text{roll}} \parallel \pi_\theta)$. Because π_{roll} logits are stored during data generation and π_θ logits are computed during the training forward pass, this quantity can be computed *exactly* without extra inference cost:

$$D_{\text{KL}}(c_t) = \sum_{v \in \mathcal{V}} \pi_{\text{roll}}(v|c_t) \log \frac{\pi_{\text{roll}}(v|c_t)}{\pi_\theta(v|c_t)}. \quad (51)$$

This eliminates the high variance associated with sample-based estimators used in standard PPO.

Masking Criterion. We employ a max-based criterion $M(x, y) = \mathbb{I}[\max_t D_{\text{KL}}(c_t) \leq \delta]$. This choice directly bounds $D_{\text{KL}}^{\text{tok}, \text{max}}$, ensuring the preconditions for our theoretical bounds are met. A key property of this criterion is *length-invariance*: unlike sum-based constraints, the threshold δ does not need to be adjusted as sequence length T grows. In practice, to tolerate occasional outliers while maintaining robustness, one may combine this with an average-based constraint: $\frac{1}{T} \sum_t D_{\text{KL}}(c_t) \leq \delta_{\text{avg}}$.

Sample-based Approximation. In memory-constrained settings where storing full rollout logits is infeasible, one must rely on sample-based estimates derived from the importance ratio ρ_t . We recommend distinct criteria:

1. **Max-Criterion (k_2):** We recommend the symmetric estimator $f(\rho) = \frac{1}{2}(\log \rho)^2$. This metric detects divergence symmetrically, flagging both support collapse ($\rho \rightarrow 0$) and impulse noise ($\rho \rightarrow \infty$) equally.
2. **Average-Criterion (k_3):** We recommend the estimator $f(\rho) = \rho - 1 - \log \rho$. This estimator is preferred because it is strictly non-negative and *unbiased* ($\mathbb{E}[f(\rho)] = D_{\text{KL}}$), ensuring that the sample average converges to the true sequence KL.

We provide a more detailed explanation in Appendix B.

6.3 Theoretical Guarantees

We formalize the properties of TRM in Theorem 6.1. By enforcing the trust region via rejection rather than penalty, TRM ensures the approximation error remains within the non-vacuous bounds derived in Section 4.

Theorem 6.1 (TRM Guarantee). *Algorithm 1 with exact KL computation and threshold δ satisfies:*

1. **Bounded Divergence:** For all accepted sequences (where $M = 1$), $\max_t D_{\text{KL}}(c_t) \leq \delta$.
2. **Length-Invariant Threshold:** The validity of the bound depends only on δ , not sequence length T .
3. **Non-Vacuous Error Bound:** If additionally $D_{\text{KL}}^{\text{tok},\max} \leq \delta$ holds globally (i.e., for all reachable contexts, not just those observed in the batch), then:

$$|J(\pi_\theta) - J(\pi_{\text{roll}}) - L(\pi_\theta)| \leq \min \{B_{\text{PM}}(\delta), B_{\text{Mix}}(\delta), B_{\text{Adap}}(\delta)\},$$

where B_{PM} , B_{Mix} , B_{Adap} are as in Eqs. (43)–(45) with $D_{\text{KL}}^{\text{tok},\max}$ replaced by δ , and L is the full (unmasked) surrogate. Writing $B(\delta) := \min\{B_{\text{PM}}(\delta), B_{\text{Mix}}(\delta), B_{\text{Adap}}(\delta)\}$, the condition $L(\pi_\theta) > B(\delta)$ guarantees monotonic improvement: $J(\pi_\theta) > J(\pi_{\text{roll}})$.

Proof. (1) **Bounded Divergence:** By construction of Algorithm 1, $M_i = 1$ only if $\max_t D_{\text{KL}}(c_t^{(i)}) \leq \delta$. Thus, for all accepted sequences, $\max_t D_{\text{KL}}(c_t) \leq \delta$.

(2) **Length-Invariant Threshold:** The masking criterion $\max_t D_{\text{KL}}(c_t) \leq \delta$ depends only on the per-token maximum, not on any sum over T . Hence, δ is a fixed constant independent of sequence length.

(3) **Non-Vacuous Error Bound:** When $D_{\text{KL}}^{\text{tok},\max} \leq \delta$ globally, Theorems 4.4, 4.5, and 4.6 apply directly:

$$|J(\pi_\theta) - J(\pi_{\text{roll}}) - L(\pi_\theta)| \leq \min \{B_{\text{PM}}(\delta), B_{\text{Mix}}(\delta), B_{\text{Adap}}(\delta)\}.$$

Since $J(\pi_\theta) - J(\pi_{\text{roll}}) \geq L(\pi_\theta) - B(\delta)$, $L(\pi_\theta) > B(\delta)$ implies $J(\pi_\theta) > J(\pi_{\text{roll}})$. \square

Remark 6.2 (Role of masking in the guarantee). *The error bound in Part (3) involves the full surrogate L , while TRM computes the masked surrogate $L_{\text{masked}} = L - L_{\text{rej}}$, where $L_{\text{rej}} = \mathbb{E}_{\pi_{\text{roll}}}[(1 - M) \cdot A \cdot \sum_t \rho_t]$ denotes the contribution from rejected sequences. TRM serves two complementary roles:*

1. **Verification:** A high acceptance rate (most sampled trajectories satisfy $\max_t D_{\text{KL}}(c_t) \leq \delta$) provides empirical evidence that $D_{\text{KL}}^{\text{tok},\max} \leq \delta$ holds globally, validating the precondition of Part (3).
2. **Robust gradient estimation:** By discarding trajectories with large importance ratios, the masked gradient ∇L_{masked} avoids the erroneous, high-variance updates from mismatched data (cf. Section 5). When the acceptance rate is high, $L_{\text{masked}} \approx L$, so $L_{\text{masked}} > B(\delta)$ approximately guarantees monotonic improvement.

We recommend monitoring the acceptance rate: a rate above 70% provides reasonable confidence that $D_{\text{KL}}^{\text{tok},\max} \approx \delta$ and $L_{\text{masked}} \approx L$.

Numerical Illustration. Revisiting the scenario from Table 1 ($T = 4096$, $\delta = 10^{-4}$), when $D_{\text{KL}}^{\text{tok},\max} \leq \delta$ holds globally, the error is bounded by **8.2** (Mixed bound) or **35.0** (Pinsker-Marginal). This contrasts sharply with the classical bound of **1677**, confirming that TRM—by enforcing and verifying this condition—provides the first theoretically grounded optimization path for long-horizon LLM reasoning.

Length bias and length-neutral extensions. While the TRM masking criterion $\max_t D_{\text{KL}}(c_t) \leq \delta$ is length-invariant in its *threshold*, the *probability of rejection* can increase with sequence length T because longer sequences have more tokens that could individually violate the threshold. This may introduce a systematic bias against longer responses in practice. In Appendix D, we propose a length-neutral variant (LN-TRM) that mitigates this concern using normalized position-aware error scores derived from the Adaptive bound, while preserving the theoretical guarantees up to controlled relaxation factors.

7 Experiments

In this section, we provide empirical evidence validating the effectiveness of our Trust Region Masking (TRM). We conduct experiments on mathematical reasoning using the vanilla Qwen3-8B-Base model under Zero-RL setup [Guo et al., 2025]. The training dataset is a deduplicated version of DAPO-MATH-17k, and evaluation is performed on the AIME25 benchmark. We utilize GRPO [Shao et al., 2024] for advantage approximation with group size 16. The train batch size and rollout batch size are both set to 32, with a learning rate of 1×10^{-6} . For robust evaluation, we use sampling parameters Top-P = 0.95 and Temperature = 1.0, reporting the avg@32 score.

To simulate a realistic, high-throughput training environment, we introduce backend discrepancies by using vLLM for the inference (rollout) engine and PyTorch FSDP for the training engine. As discussed in Appendix A, the accumulation of floating-point differences between these backends acts as a primary source of off-policy divergence. To explicitly measure this mismatch between the rollout policy π_{roll} and the training policy π_θ during the update phase, we define the *Log Absolute Perplexity (PPL) Gap*. For a batch size N , this is calculated as:

$$\Delta_{\text{PPL}} = \frac{1}{N} \sum_{i=1}^N \left| \frac{1}{T_i} \sum_{t=1}^{T_i} \log \pi_\theta(y_t^{(i)} | c_t^{(i)}) - \frac{1}{T_i} \sum_{t=1}^{T_i} \log \pi_{\text{roll}}(y_t^{(i)} | c_t^{(i)}) \right|. \quad (52)$$

This metric quantifies the average per-token log-probability drift attributable to backend discrepancies.

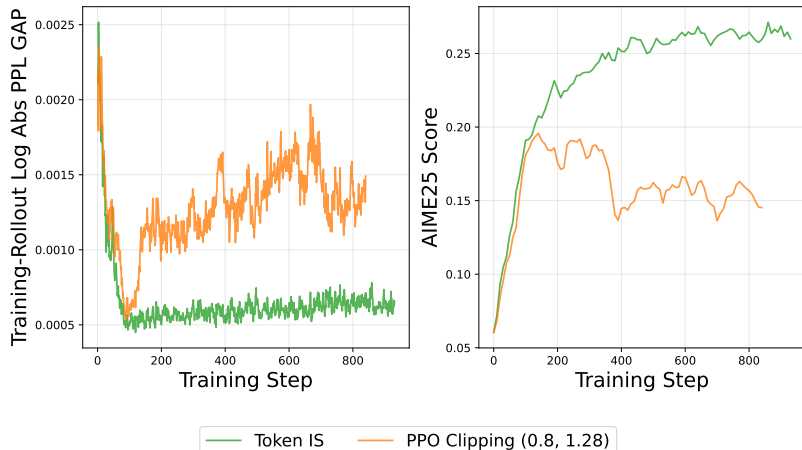


Figure 1: Comparison of Token IS and PPO Clipping.

We first compare original Token-level Importance Sampling (Token IS) against Token-level PPO Clipping. For the clipping method, we adopt the range settings from DAPO [Yu et al., 2025], clipping

ratios to $[0.8, 1.28]$. As shown in Figure 1, token-level PPO Clipping exacerbates training instability, resulting in a significantly larger PPL Gap and degraded performance. This empirical finding aligns with our analysis in Section 5: standard token-level interventions are mathematically insufficient to control $D_{\text{KL}}^{\text{tok},\text{max}}$ —a property of the *entire sequence*. Consequently, they fail to prevent optimization collapse when faced with off-policy mismatch.

Then we demonstrate the effectiveness of our proposed sequence-level method, TRM. We compare TRM against standard PPO Clipping using two variants: **TRM-Max**, which masks sequences using a threshold $\delta = 0.05$, and **TRM-Avg**, which uses a threshold $\delta = 0.001$.

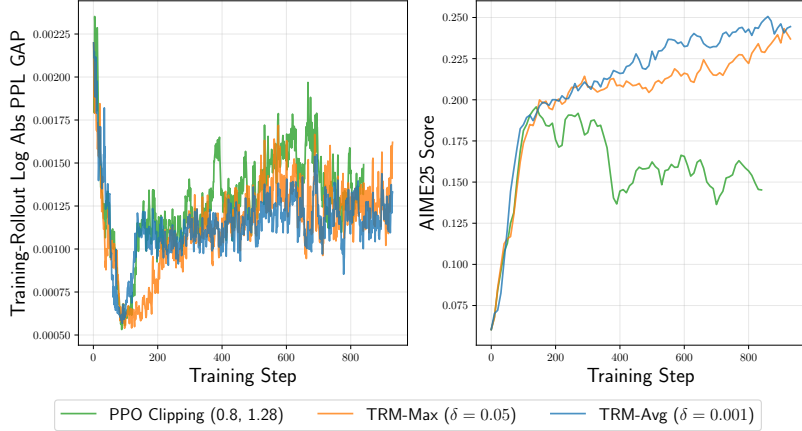


Figure 2: Empirical comparison between TRM and standard PPO Clipping.

As illustrated in Figure 2, standard PPO Clipping fails to prevent collapse; the validation score degrades rapidly as the training progresses, correlating with an explosion in the PPL Gap. This confirms our theoretical finding in Section 5 that token-level clipping allows gradient leakage from mismatched trajectories. In contrast, both TRM variants maintain training stability. By rejecting entire sequences where implementation divergence exceeds the trust region, TRM keeps the PPL Gap bounded and ensures consistent improvement on the AIME25 benchmark.

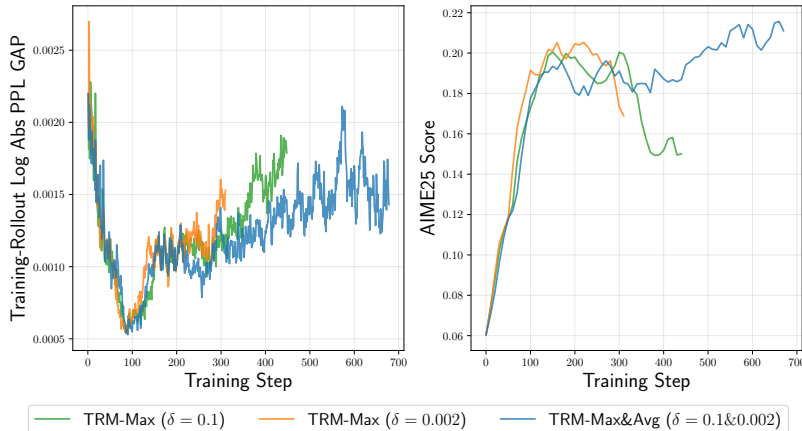


Figure 3: Effectiveness of Combined Criterion.

In practice, one can also apply both Max and Avg criteria simultaneously, which allows for the use of looser thresholds. As demonstrated in Figure 3, while TRM-Max (with $\delta = 0.1$) and TRM-Avg

(with $\delta = 0.002$) individually fail to prevent training collapse due to the relaxed constraints, their combination (TRM-Max&Avg) successfully stabilizes training. This suggests that the two criteria are complementary: the max constraint catches extreme outliers, while the average constraint limits accumulated drift. Therefore, we recommend monitoring health metrics such as the Log Absolute PPL Gap to determine the appropriate criterion and thresholds when deploying TRM in real-world applications.

8 Conclusion and Discussion

Off-policy mismatch is unavoidable in modern LLM-RL due to implementation divergence. We show that classical trust region bounds, scaling as $O(T^2)$, become theoretically vacuous for long-horizon tasks common in reasoning domains. By deriving the Pinsker-Marginal bound ($O(T^{3/2})$), the Mixed bound ($O(T)$), and the Adaptive bound (which strictly generalizes the Pinsker-Marginal bound via a trajectory-level importance-ratio decomposition with per-position Pinsker application), we establish that valid policy improvement depends strictly on the *maximum* token-level divergence—a quantity uncontrollable by standard token-level clipping. The minimum over all three bounds is tighter than any individual bound across divergence regimes. Consequently, we propose Trust Region Masking (TRM), a sequence-level intervention that masks entire sequences violating trust region constraints, thereby enabling the first non-vacuous monotonic improvement guarantees for long-horizon LLM-RL.

Our analysis extends beyond the specific algorithm proposed here, applying to any method utilizing the standard surrogate objective, including REINFORCE and various PPO derivatives. The fundamental insight—that trust region constraints must be enforced at the sequence level rather than the token level—is universal for autoregressive generation. While the strict max-criterion used in TRM ensures theoretical rigor, it can be aggressive in high-noise regimes. The average-criterion offers a pragmatic relaxation, trading some theoretical tightness for improved sample efficiency. We additionally identify *length bias* as a practical concern for any sequence-level masking method and propose length-neutral extensions in Appendix D. We recommend that practitioners monitor the off-policy mismatch gap, masking rate, and length-stratified rejection rates as diagnostic tools. In future work, we will explore tighter bounds by leveraging distributional information beyond bounded reward assumptions, as well as adaptive thresholds and soft masking (e.g., importance weighting) to further enhance stability in complex agentic workflows.

References

Joshua Achiam, David Held, Aviv Tamar, and Pieter Abbeel. Constrained policy optimization. In *International conference on machine learning*, pages 22–31. PMLR, 2017.

Samy Bengio, Oriol Vinyals, Navdeep Jaitly, and Noam Shazeer. Scheduled sampling for sequence prediction with recurrent neural networks. *Advances in neural information processing systems*, 28, 2015.

Thomas M Cover. *Elements of information theory*. John Wiley & Sons, 1999.

Lasse Espeholt, Hubert Soyer, Remi Munos, Karen Simonyan, Vlad Mnih, Tom Ward, Yotam Doron, Vlad Firoiu, Tim Harley, Iain Dunning, et al. Impala: Scalable distributed deep-rl with importance weighted actor-learner architectures. In *International conference on machine learning*, pages 1407–1416. PMLR, 2018.

Qiuhan Gu. Llm-based code generation method for golang compiler testing. In *Proceedings of the 31st ACM Joint European Software Engineering Conference and Symposium on the Foundations of Software Engineering*, pages 2201–2203, 2023.

Daya Guo, Dejian Yang, Haowei Zhang, Junxiao Song, Ruoyu Zhang, Runxin Xu, Qihao Zhu, Shirong Ma, Peiyi Wang, Xiao Bi, et al. Deepseek-r1: Incentivizing reasoning capability in llms via reinforcement learning. *arXiv preprint arXiv:2501.12948*, 2025.

Sham Kakade and John Langford. Approximately optimal approximate reinforcement learning. In *Proceedings of the nineteenth international conference on machine learning*, pages 267–274, 2002.

Woosuk Kwon, Zhuohan Li, Siyuan Zhuang, Ying Sheng, Lianmin Zheng, Cody Hao Yu, Joseph Gonzalez, Hao Zhang, and Ion Stoica. Efficient memory management for large language model serving with pagedattention. In *Proceedings of the 29th symposium on operating systems principles*, pages 611–626, 2023.

Hunter Lightman, Vineet Kosaraju, Yuri Burda, Harrison Edwards, Bowen Baker, Teddy Lee, Jan Leike, John Schulman, Ilya Sutskever, and Karl Cobbe. Let’s verify step by step. In *The Twelfth International Conference on Learning Representations*, 2023.

Aixin Liu, Bei Feng, Bin Wang, Bingxuan Wang, Bo Liu, Chenggang Zhao, Chengqi Dengr, Chong Ruan, Damai Dai, Daya Guo, et al. Deepseek-v2: A strong, economical, and efficient mixture-of-experts language model. *arXiv preprint arXiv:2405.04434*, 2024a.

Fang Liu, Yang Liu, Lin Shi, Houkun Huang, Ruifeng Wang, Zhen Yang, Li Zhang, Zhongqi Li, and Yuchi Ma. Exploring and evaluating hallucinations in llm-powered code generation. *arXiv preprint arXiv:2404.00971*, 2024b.

Jiacai Liu, Yingru Li, Yuqian Fu, Jiawei Wang, Qian Liu, and Yu Shen. When speed kills stability: Demystifying RL collapse from the training-inference mismatch, 2025. URL <https://richardli.xyz/rl-collapse>.

Arun Nair, Praveen Srinivasan, Sam Blackwell, Cagdas Alcicek, Rory Fearon, Alessandro De Maria, Vedavyas Panneershelvam, Mustafa Suleyman, Charles Beattie, Stig Petersen, et al. Massively parallel methods for deep reinforcement learning. *arXiv preprint arXiv:1507.04296*, 2015.

Mark S Pinsker. Information and information stability of random variables and processes. *Holden-Day*, 1964.

Penghui Qi, Xiangxin Zhou, Zichen Liu, Tianyu Pang, Chao Du, Min Lin, and Wee Sun Lee. Rethinking the trust region in llm reinforcement learning, 2026. URL <https://arxiv.org/abs/2602.04879>.

John Schulman, Sergey Levine, Pieter Abbeel, Michael Jordan, and Philipp Moritz. Trust region policy optimization. In *International conference on machine learning*, pages 1889–1897. PMLR, 2015.

John Schulman, Filip Wolski, Prafulla Dhariwal, Alec Radford, and Oleg Klimov. Proximal policy optimization algorithms. *arXiv preprint arXiv:1707.06347*, 2017.

Zhihong Shao, Peiyi Wang, Qihao Zhu, Runxin Xu, Junxiao Song, Xiao Bi, Haowei Zhang, Mingchuan Zhang, YK Li, Yang Wu, et al. Deepseekmath: Pushing the limits of mathematical reasoning in open language models. *arXiv preprint arXiv:2402.03300*, 2024.

Noam Shazeer, Azalia Mirhoseini, Krzysztof Maziarz, Andy Davis, Quoc Le, Geoffrey Hinton, and Jeff Dean. Outrageously large neural networks: The sparsely-gated mixture-of-experts layer. *arXiv preprint arXiv:1701.06538*, 2017.

Mohammad Shoeybi, Mostofa Patwary, Raul Puri, Patrick LeGresley, Jared Casper, and Bryan Catanzaro. Megatron-lm: Training multi-billion parameter language models using model parallelism. *arXiv preprint arXiv:1909.08053*, 2019.

Richard S Sutton, David McAllester, Satinder Singh, and Yishay Mansour. Policy gradient methods for reinforcement learning with function approximation. *Advances in neural information processing systems*, 12, 1999.

Ronald J Williams. Simple statistical gradient-following algorithms for connectionist reinforcement learning. *Machine learning*, 8(3):229–256, 1992.

John Yang, Carlos E Jimenez, Alexander Wettig, Kilian Lieret, Shunyu Yao, Karthik Narasimhan, and Ofir Press. Swe-agent: Agent-computer interfaces enable automated software engineering. *Advances in Neural Information Processing Systems*, 37:50528–50652, 2024.

Feng Yao, Liyuan Liu, Dinghuai Zhang, Chengyu Dong, Jingbo Shang, and Jianfeng Gao. Your efficient rl framework secretly brings you off-policy rl training, 2025. URL <https://fengyao.notion.site/off-policy-rl>.

Qiyi Yu, Zheng Zhang, Ruofei Zhu, Yufeng Yuan, Xiaochen Zuo, Yu Yue, Weinan Dai, Tiantian Fan, Gaohong Liu, Lingjun Liu, et al. Dapo: An open-source llm reinforcement learning system at scale. *arXiv preprint arXiv:2503.14476*, 2025.

Weihao Zeng, Yuzhen Huang, Qian Liu, Wei Liu, Keqing He, Zejun Ma, and Junxian He. Simplerl-zoo: Investigating and taming zero reinforcement learning for open base models in the wild. *arXiv preprint arXiv:2503.18892*, 2025.

Yanli Zhao, Andrew Gu, Rohan Varma, Liang Luo, Chien-Chin Huang, Min Xu, Less Wright, Hamid Shojanazeri, Myle Ott, Sam Shleifer, et al. Pytorch fsdp: experiences on scaling fully sharded data parallel. *arXiv preprint arXiv:2304.11277*, 2023.

Lianmin Zheng, Liangsheng Yin, Zhiqiang Xie, Chuyue Livia Sun, Jeff Huang, Cody Hao Yu, Shiyi Cao, Christos Kozyrakis, Ion Stoica, Joseph E Gonzalez, et al. Sclang: Efficient execution of structured language model programs. *Advances in neural information processing systems*, 37: 62557–62583, 2024.

Daniel M Ziegler, Nisan Stiennon, Jeffrey Wu, Tom B Brown, Alec Radford, Dario Amodei, Paul Christiano, and Geoffrey Irving. Fine-tuning language models from human preferences. *arXiv preprint arXiv:1909.08593*, 2019.

A Details on Off-Policy Mismatch in LLM-RL

Prior work has established that off-policy mismatch ($\pi_{\text{roll}} \neq \pi_{\theta}$) is unavoidable in modern LLM-RL pipelines due to system-level constraints [Liu et al., 2025, Yao et al., 2025]. Here, we detail the specific sources of this divergence.

A.1 Backend Discrepancies

To maximize throughput, modern LLM infrastructures employ distinct software stacks for inference and training [Kwon et al., 2023, Zheng et al., 2024, Shoeybi et al., 2019]. These differences are summarized below:

Inference (vLLM/SGLang)	Training (Megatron/FSDP)
PagedAttention	FlashAttention-2
FP8/INT8 KV-cache quantization	BF16/FP32 accumulation
Aggressive operator fusion	Tensor parallelism

Floating-point Non-associativity. The root cause of divergence is the non-associativity of floating-point arithmetic: $(a \oplus b) \oplus c \neq a \oplus (b \oplus c)$. In attention mechanisms, the softmax denominator requires reducing over the context length. Different parallel reduction orders yield slightly different denominators. While these errors are negligible for a single token, they compound autoregressively over T steps, leading to significant trajectory divergence.

A.2 Mixture-of-Experts (MoE) Routing Discontinuities

In MoE architectures [Shazeer et al., 2017, Liu et al., 2024a], the output is computed as:

$$y = \sum_{i \in \mathcal{K}} g_i(x) \cdot E_i(x), \quad \mathcal{K} = \text{Top-K}(h(x)), \quad (53)$$

where $h(x)$ represents the router logits. The Top-K operator is *discontinuous*. If numerical precision differences cause a shift $h_{\text{inf}} = h_{\text{train}} + \epsilon$ such that $|h_{(K)} - h_{(K+1)}| < \|\epsilon\|$, the set of selected experts \mathcal{K} changes.

Support Collapse. A change in expert selection can drastically alter the output distribution. For instance, if $\pi_{\text{roll}}(\text{"apple"}) = 0.9$ but a routing flip causes $\pi_{\theta}(\text{"apple"}) \approx 0.001$, the importance ratio spikes to $\rho \approx 900$. This creates *impulse noise* in the gradient estimator, destabilizing training.

A.3 Distributed Staleness

Large-scale training typically employs a decoupled actor-learner architecture [Espeholt et al., 2018, Nair et al., 2015]:

- **Actors** generate rollouts using parameters θ_{old} .
- **Learner** updates parameters to θ_{new} .
- **Latency** introduces a lag of k gradient steps between generation and consumption.

Consequently, $\theta_{\text{train}} = \theta_{\text{rollout}} + \sum_{i=1}^k \Delta\theta_i$, ensuring $\pi_{\text{roll}} \neq \pi_{\theta}$ even if implementations were identical.

Summary. These factors render off-policy mismatch *systemic* rather than incidental. Robust theoretical bounds must therefore account for $\pi_{\text{roll}} \neq \pi_{\theta}$ explicitly.

B Sample-Based Estimators (k_2 and k_3)

In settings where storing full logits is infeasible, we rely on sample-based estimators computed from the importance ratio $\rho_t = \pi_{\theta}(y_t|c_t)/\pi_{\text{roll}}(y_t|c_t)$. We analyze two estimators: k_3 (for unbiased averaging) and k_2 (for symmetric max-filtering).

B.1 The k_3 Estimator for Averaging

The k_3 estimator is defined as $f(\rho) = \rho - 1 - \log \rho$.

- **Unbiased:** It is the only estimator where $\mathbb{E}_{y \sim \pi_{\text{roll}}}[k_3(\rho)] = D_{\text{KL}}(\pi_{\text{roll}} \parallel \pi_{\theta})$ exactly. This makes it ideal for the *average-based criterion* $\frac{1}{T} \sum k_3$, as the sample mean converges to the true sequence KL by the Law of Large Numbers.
- **Non-negative:** $k_3 \geq 0$ for all ρ , preventing cancellation artifacts common with simple log-ratios.
- **Asymmetric:** The k_3 estimator penalizes $\rho \gg 1$ much more heavily than $\rho \ll 1$. This is correct for averaging (since high ρ values are rare under π_{roll}), but makes it poor for detecting single-token outliers.

B.2 The k_2 Estimator for Max-Filtering

The k_2 estimator is defined as $f(\rho) = \frac{1}{2}(\log \rho)^2$. This is the second-order Taylor approximation of the KL divergence.

- **Symmetric:** $k_2(\rho) = k_2(1/\rho)$. It penalizes deviations in either direction equally.
- **Robustness:** For the *max-based criterion*, we require a detector that flags both “support collapse” (where $\pi_{\theta} \ll \pi_{\text{roll}}$, $\rho \rightarrow 0$) and “impulse noise” (where $\pi_{\theta} \gg \pi_{\text{roll}}$, $\rho \rightarrow \infty$). The k_3 estimator fails to flag $\rho \rightarrow 0$ aggressively (e.g., $k_3(0.01) \approx 3.6$), whereas k_2 treats it symmetrically to $\rho = 100$ ($k_2 \approx 10.6$).
- **Usage:** We recommend k_2 specifically for the max-threshold check: $M_i = \mathbb{I}[\max_t k_2(\rho_t) \leq \delta]$.

Caveat. Both k_2 and k_3 are single-sample approximations. While effective heuristics, the rigorous guarantees of Theorem 6.1 hold only when using the exact KL computed from full logits.

C Proof of the Adaptive Bound

We provide the full proof of Theorem 4.6, which combines an importance-ratio decomposition of the error with an adaptive per-position application of Pinsker’s inequality.

C.1 The Importance-Ratio Error Decomposition

We begin from an exact identity for the error. Let $\mu = \pi_{\text{roll}}$ and $\pi = \pi_\theta$ for brevity. The surrogate can be written as:

$$L'_\mu(\pi) = \mathbb{E}_{y \sim \mu} \left[R(y) \sum_{t=1}^T \left(\frac{\pi_t}{\mu_t} - 1 \right) \right], \quad (54)$$

where $\pi_t := \pi(y_t | c_t)$, $\mu_t := \mu(y_t | c_t)$, and $R(y) \in [0, 1]$.

Lemma C.1 (Exact Error Identity). *The performance difference satisfies:*

$$J(\pi) - J(\mu) = L'_\mu(\pi) - \Delta(\mu, \pi), \quad (55)$$

where:

$$\Delta(\mu, \pi) = \mathbb{E}_{y \sim \mu} \left[R(y) \sum_{t=1}^T \left(\frac{\pi_t}{\mu_t} - 1 \right) \left(1 - \prod_{j=t+1}^T \frac{\pi_j}{\mu_j} \right) \right]. \quad (56)$$

Proof. We verify this algebraic identity. Using the telescoping decomposition of the full importance weight:

$$\prod_{t=1}^T \rho_t - 1 = \sum_{t=1}^T (\rho_t - 1) \prod_{j=t+1}^T \rho_j, \quad (57)$$

the true performance difference is:

$$J(\pi) - J(\mu) = \mathbb{E}_{y \sim \mu} \left[R(y) \left(\prod_{t=1}^T \rho_t - 1 \right) \right] = \mathbb{E}_{y \sim \mu} \left[R(y) \sum_{t=1}^T (\rho_t - 1) \prod_{j>t} \rho_j \right]. \quad (58)$$

The surrogate is $L'_\mu(\pi) = \mathbb{E}_{y \sim \mu} [R(y) \sum_t (\rho_t - 1)]$. Subtracting:

$$J(\pi) - J(\mu) - L'_\mu(\pi) = \mathbb{E}_{y \sim \mu} \left[R(y) \sum_t (\rho_t - 1) \left(\prod_{j>t} \rho_j - 1 \right) \right] = -\Delta(\mu, \pi). \quad (59)$$

Hence $J(\pi) - J(\mu) = L'_\mu(\pi) - \Delta(\mu, \pi)$, and $|\text{Error}| = |\Delta|$. \square

C.2 Factoring via the Tower Property

For each summand in Eq. (56), define:

$$A_t := \left| \frac{\pi_t}{\mu_t} - 1 \right|, \quad B_t := \left| 1 - \prod_{j=t+1}^T \frac{\pi_j}{\mu_j} \right|. \quad (60)$$

Since $|R(y)| \leq 1$, the triangle inequality gives:

$$|\Delta| \leq \mathbb{E}_{y \sim \mu} \left[\sum_{t=1}^T A_t \cdot B_t \right]. \quad (61)$$

The crucial observation is that A_t depends on y_t (given c_t) while B_t depends on $y_{>t} = (y_{t+1}, \dots, y_T)$. However, they are *not* independent given c_t , because $y_{>t}$ depends on y_t through $c_{t+1} = (c_t, y_t)$. We apply the tower property by conditioning on c_{t+1} :

$$\mathbb{E}_{y \sim \mu} \left[\sum_t A_t B_t \right] = \sum_{t=1}^T \mathbb{E}_{y_{\leq t} \sim \mu} \left[A_t \cdot \mathbb{E}_{y_{>t} \sim \mu(\cdot | c_{t+1})} [B_t] \right]. \quad (62)$$

Now, the inner expectation has a clean interpretation:

$$\begin{aligned} \mathbb{E}_{y_{>t} \sim \mu(\cdot | c_{t+1})} [B_t] &= \mathbb{E}_{y_{>t} \sim \mu(\cdot | c_{t+1})} \left[\left| 1 - \frac{\pi(y_{>t} | c_{t+1})}{\mu(y_{>t} | c_{t+1})} \right| \right] \\ &= \sum_{y_{>t}} \mu(y_{>t} | c_{t+1}) \left| 1 - \frac{\pi(y_{>t} | c_{t+1})}{\mu(y_{>t} | c_{t+1})} \right| \\ &= \sum_{y_{>t}} |\mu(y_{>t} | c_{t+1}) - \pi(y_{>t} | c_{t+1})| \\ &= 2 D_{\text{TV}}(\mu_{>t}(\cdot | c_{t+1}) \| \pi_{>t}(\cdot | c_{t+1})), \end{aligned} \quad (63)$$

where $\mu_{>t}(\cdot | c_{t+1})$ and $\pi_{>t}(\cdot | c_{t+1})$ are the distributions over future trajectories (y_{t+1}, \dots, y_T) under μ and π respectively, conditioned on the context c_{t+1} .

C.3 Bounding the Future-Trajectory TV Adaptively

We now bound the future-trajectory TV distance in Eq. (63). For any fixed context c_{t+1} , we have two routes:

Route 1 (Trivial): Since TV distance is bounded by 1:

$$D_{\text{TV}}(\mu_{>t}(\cdot | c_{t+1}) \| \pi_{>t}(\cdot | c_{t+1})) \leq 1. \quad (64)$$

Route 2 (Pinsker + KL chain rule): By Pinsker's inequality applied to the joint future distribution:

$$D_{\text{TV}}(\mu_{>t}(\cdot | c_{t+1}) \| \pi_{>t}(\cdot | c_{t+1})) \leq \sqrt{\frac{1}{2} D_{\text{KL}}(\mu_{>t}(\cdot | c_{t+1}) \| \pi_{>t}(\cdot | c_{t+1}))}. \quad (65)$$

By the KL chain rule applied to the conditional future distribution:

$$D_{\text{KL}}(\mu_{>t}(\cdot | c_{t+1}) \| \pi_{>t}(\cdot | c_{t+1})) = \sum_{k=t+1}^T \mathbb{E}_{c_k \sim \mu(\cdot | c_{t+1})} [D_{\text{KL}}(c_k)] \leq (T-t) \cdot D_{\text{KL}}^{\text{tok,max}}. \quad (66)$$

The inequality follows because $D_{\text{KL}}(c_k) \leq D_{\text{KL}}^{\text{tok,max}}$ for all c_k by definition.

Combining Eq. (65) and Eq. (66):

$$D_{\text{TV}}(\mu_{>t}(\cdot | c_{t+1}) \| \pi_{>t}(\cdot | c_{t+1})) \leq \sqrt{\frac{(T-t) D_{\text{KL}}^{\text{tok,max}}}{2}}. \quad (67)$$

Taking the minimum of Eq. (64) and Eq. (67):

$$D_{\text{TV}}(\mu_{>t}(\cdot | c_{t+1}) \| \pi_{>t}(\cdot | c_{t+1})) \leq \min \left(1, \sqrt{\frac{(T-t) D_{\text{KL}}^{\text{tok,max}}}{2}} \right). \quad (68)$$

Crucially, this bound holds for *every* realization of c_{t+1} , because the worst-case replacement in Eq. (66) does not depend on the specific context. Therefore, it can be factored out of the outer expectation in Eq. (62).

C.4 Combining the Factors

Substituting Eq. (63) and Eq. (68) into Eq. (62):

$$\begin{aligned} |\Delta| &\leq \sum_{t=1}^T \mathbb{E}_{y_{\leq t} \sim \mu}[A_t] \cdot 2 \min\left(1, \sqrt{\frac{(T-t)D_{\text{KL}}^{\text{tok,max}}}{2}}\right) \\ &= 2 \sum_{t=1}^T \mathbb{E}_{c_t \sim d_t^\mu} \left[\mathbb{E}_{y_t \sim \mu(\cdot|c_t)} \left[\left| \frac{\pi_t}{\mu_t} - 1 \right| \right] \right] \cdot \min\left(1, \sqrt{\frac{(T-t)D_{\text{KL}}^{\text{tok,max}}}{2}}\right). \end{aligned} \quad (69)$$

Now, $\mathbb{E}_{y_t \sim \mu(\cdot|c_t)}[\left| \frac{\pi_t}{\mu_t} - 1 \right|] = \sum_v |\pi(v|c_t) - \mu(v|c_t)| = 2D_{\text{TV}}^{\text{tok}}(c_t)$. Therefore:

$$\mathbb{E}_{c_t \sim d_t^\mu} \left[\mathbb{E}_{y_t \sim \mu(\cdot|c_t)} \left[\left| \frac{\pi_t}{\mu_t} - 1 \right| \right] \right] = 2\bar{D}_t, \quad (70)$$

where $\bar{D}_t = \mathbb{E}_{c_t \sim d_t^\mu}[D_{\text{TV}}^{\text{tok}}(c_t)]$.

Proof of Theorem 4.6. Substituting into Eq. (69):

$$|\Delta| \leq 4 \sum_{t=1}^T \bar{D}_t \cdot \min\left(1, \sqrt{\frac{(T-t)D_{\text{KL}}^{\text{tok,max}}}{2}}\right). \quad (71)$$

Since $\text{Error} = -\Delta$ (from Lemma C.1), this gives $|\text{Error}| = |\Delta|$, completing the proof.

Strictness over Pinsker-Marginal: We show this by demonstrating that the worst-case Adaptive bound (with \bar{D}_t replaced by its upper bound) recovers the full Pinsker-Marginal bound Eq. (28). Since $\bar{D}_t \leq D_{\text{TV}}^{\text{tok,max}} \leq \min(1, \sqrt{D_{\text{KL}}^{\text{tok,max}}/2})$, and the future-trajectory TV $\min(1, \sqrt{(T-t)D_{\text{KL}}^{\text{tok,max}}/2})$ mirrors the Pinsker-Marginal's context-shift term $\min(1, \sqrt{(t-1)D_{\text{KL}}^{\text{tok,max}}/2})$ (via the index reversal $\sum_t f(T-t) = \sum_t f(t-1)$), the worst-case Adaptive bound equals the Pinsker-Marginal bound with all caps included. Since $\bar{D}_t \leq D_{\text{TV}}^{\text{tok,max}}$ with possible strict inequality, and the Adaptive bound includes the $\min(1, \cdot)$ cap on the future factor, it is at least as tight as the Pinsker-Marginal bound, and strictly tighter whenever $\bar{D}_t < D_{\text{TV}}^{\text{tok,max}}$ at some position.

Strictness over the linear bound: The linear bound corresponds to setting the future TV to its trivial upper bound of 1 at every position: $|\Delta| \leq 4 \sum_t \bar{D}_t$. The Adaptive bound replaces 1 with $\min(1, \sqrt{(T-t)D_{\text{KL}}^{\text{tok,max}}/2})$, which is ≤ 1 always and < 1 whenever $(T-t)D_{\text{KL}}^{\text{tok,max}}/2 < 1$, i.e., for positions $t > T - 2/D_{\text{KL}}^{\text{tok,max}}$. \square

C.5 Worst-Case Evaluation

When $\bar{D}_t = D_{\text{TV}}^{\text{tok,max}}$ for all t (uniform divergence), the Adaptive bound becomes:

$$|\text{Error}| \leq 4D_{\text{TV}}^{\text{tok,max}} \sum_{t=1}^T \min\left(1, \sqrt{\frac{(T-t)D_{\text{KL}}^{\text{tok,max}}}{2}}\right). \quad (72)$$

Using $D_{\text{TV}}^{\text{tok,max}} \leq \min(1, \sqrt{D_{\text{KL}}^{\text{tok,max}}/2})$ and evaluating the sum in two regimes defined by the crossover point $t^* = T - \lfloor 2/D_{\text{KL}}^{\text{tok,max}} \rfloor$:

Case 1: $2/D_{\text{KL}}^{\text{tok},\text{max}} > T$ (small divergence). All terms satisfy $(T-t)D_{\text{KL}}^{\text{tok},\text{max}}/2 < 1$, so $\min = \sqrt{(T-t)D_{\text{KL}}^{\text{tok},\text{max}}/2}$ throughout. Also $D_{\text{KL}}^{\text{tok},\text{max}} < 2/T < 2$, so $D_{\text{TV}}^{\text{tok},\text{max}} \leq \sqrt{D_{\text{KL}}^{\text{tok},\text{max}}/2}$ (Pinsker branch active):

$$\text{Sum} = \sqrt{\frac{D_{\text{KL}}^{\text{tok},\text{max}}}{2}} \sum_{k=0}^{T-1} \sqrt{k} \leq \sqrt{\frac{D_{\text{KL}}^{\text{tok},\text{max}}}{2}} \cdot \frac{2}{3} T^{3/2}. \quad (73)$$

Multiplied by $4\sqrt{D_{\text{KL}}^{\text{tok},\text{max}}/2}$: $|\text{Error}| \leq \frac{4}{3}T^{3/2}D_{\text{KL}}^{\text{tok},\text{max}}$, recovering the simplified Pinsker-Marginal bound Eq. (29) exactly.

Case 2: $2/D_{\text{KL}}^{\text{tok},\text{max}} \leq T$ (moderate/large divergence). For $t \leq t^*$, the min saturates at 1, contributing $t^* = T - \lfloor 2/D_{\text{KL}}^{\text{tok},\text{max}} \rfloor$ terms. For $t > t^*$, the Pinsker branch is active. The total is:

$$\text{Sum} \leq \left(T - \frac{2}{D_{\text{KL}}^{\text{tok},\text{max}}} \right) + \sqrt{\frac{D_{\text{KL}}^{\text{tok},\text{max}}}{2}} \cdot \frac{2}{3} \left(\frac{2}{D_{\text{KL}}^{\text{tok},\text{max}}} \right)^{3/2} = \left(T - \frac{2}{D_{\text{KL}}^{\text{tok},\text{max}}} \right) + \frac{4}{3D_{\text{KL}}^{\text{tok},\text{max}}}. \quad (74)$$

The prefactor is $4 \min(1, \sqrt{D_{\text{KL}}^{\text{tok},\text{max}}/2})$:

- If additionally $D_{\text{KL}}^{\text{tok},\text{max}} < 2$: prefactor = $4\sqrt{D_{\text{KL}}^{\text{tok},\text{max}}/2}$, and the bound becomes $4\sqrt{D_{\text{KL}}^{\text{tok},\text{max}}/2}[(T - 2/D_{\text{KL}}^{\text{tok},\text{max}}) + 4/(3D_{\text{KL}}^{\text{tok},\text{max}})]$.
- If $D_{\text{KL}}^{\text{tok},\text{max}} \geq 2$: prefactor = 4, and the bound becomes $4[(T - 2/D_{\text{KL}}^{\text{tok},\text{max}}) + 4/(3D_{\text{KL}}^{\text{tok},\text{max}})]$.

For $D_{\text{KL}}^{\text{tok},\text{max}} = 0.01$ (a moderate divergence where $2/D_{\text{KL}}^{\text{tok},\text{max}} = 200 < T$), $T = 4096$: $\text{Sum} \leq (4096 - 200) + 133 = 4029$, prefactor = $4\sqrt{0.005} \approx 0.283$, giving $|\text{Error}| \leq 0.283 \cdot 4029 \approx 1139$. Compare to simplified Pinsker-Marginal: $\frac{4}{3}(4096)^{3/2}(0.01) \approx 3495$, a $3 \times$ improvement.

D Length-Neutral Trust Region Masking

While TRM’s max-criterion $\max_t D_{\text{KL}}(c_t) \leq \delta$ is length-invariant in its *threshold*, the *probability of rejection* can increase with sequence length T . Intuitively, longer sequences have more tokens, each of which could individually violate the threshold, so the probability that at least one token exceeds δ grows with T . In this appendix, we formalize this concern and propose length-neutral extensions motivated by the Adaptive bound.

D.1 Quantifying Length Bias in TRM

To make the argument precise, suppose per-token KL divergences are i.i.d. draws from some distribution \mathcal{F} with $\Pr_{\mathcal{F}}[D_{\text{KL}}(c_t) > \delta] = p$. This is a simplifying assumption (in practice, divergences are correlated through the shared prefix), but it captures the essential scaling behavior.

The acceptance probability of a length- T sequence under TRM-Max is:

$$\Pr[\text{accept}] = \Pr \left[\max_t D_{\text{KL}}(c_t) \leq \delta \right] = (1-p)^T. \quad (75)$$

For small p and large T , this is approximately e^{-pT} , which decays exponentially with T . Concretely:

T	256	1024	4096	8192	16384
$(1-p)^T$ at $p = 10^{-3}$	0.774	0.358	0.017	0.0003	$< 10^{-7}$
$(1-p)^T$ at $p = 10^{-4}$	0.975	0.903	0.663	0.440	0.194

This confirms that TRM-Max systematically rejects long sequences.

Remark D.1 (Practical consequences for reasoning). *For RL training of reasoning models, length bias is particularly concerning because correct solutions often require longer chains of thought. If TRM systematically rejects long sequences, it may inadvertently incentivize the model to produce shorter (potentially less thorough) responses. Monitoring the acceptance rate stratified by sequence length is therefore essential.*

D.2 Adaptive Error Score

Motivated by the Adaptive bound (Theorem 4.6), we define a trajectory-level error score that reflects the actual per-trajectory contribution to the approximation error. For a trajectory y of length T with importance ratios ρ_t , define:

$$W(y) := \sum_{t=1}^T |\rho_t - 1| \cdot \min\left(1, \sqrt{\frac{(T-t)\delta}{2}}\right), \quad (76)$$

where δ is the per-token KL tolerance (controlling $D_{\text{KL}}^{\text{tok},\max}$). The position weight $\min(1, \sqrt{(T-t)\delta/2})$ directly reflects the future-trajectory TV bound from Eq. (68): early tokens (small t , large $T-t$) have larger weights because divergence there propagates through all subsequent tokens.

D.3 Length-Neutral TRM (LN-TRM)

The raw score $W(y)$ in Eq. (76) is a sum over T terms and therefore grows with T even when per-token divergence is constant. To obtain a length-neutral criterion, we normalize by the sum of position weights:

Definition D.2 (Normalized Error Score).

$$\widetilde{W}(y) := \frac{W(y)}{Z(T)}, \quad \text{where} \quad Z(T) := \sum_{t=1}^T \min\left(1, \sqrt{\frac{(T-t)\delta}{2}}\right). \quad (77)$$

The normalization factor $Z(T)$ depends only on T and δ , so it can be precomputed. Crucially, $\widetilde{W}(y)$ is a *weighted average* of per-token ratio deviations $|\rho_t - 1|$, making it approximately length-invariant: if per-token divergence is constant across lengths, \widetilde{W} is constant regardless of T .

D.4 Theoretical Guarantee for LN-TRM

LN-TRM trades exact control of $W(y)$ for length neutrality. The following proposition establishes the resulting guarantee.

Proposition D.3 (LN-TRM Guarantee). *Under Algorithm 2 with per-token KL tolerance δ :*

1. **Per-trajectory score bound:** For all accepted sequences ($M_i = 1$):

$$W(y^{(i)}) \leq \delta_W \cdot Z(T_i). \quad (78)$$

Algorithm 2 Length-Neutral Trust Region Masking (LN-TRM)

Require: Per-token KL tolerance δ ; Error budget δ_W ; Batch $\mathcal{D} = \{(x^{(i)}, y^{(i)})\}_{i=1}^N$

- 1: **for** each distinct length T in the batch **do**
- 2: Precompute $Z(T) \leftarrow \sum_{t=1}^T \min(1, \sqrt{(T-t)\delta/2})$
- 3: **end for**
- 4: **Forward Pass:** Compute logits for π_θ on all data
- 5: **for** each sequence i with length T_i **do**
- 6: Compute $\rho_t^{(i)} \leftarrow \pi_\theta(y_t^{(i)} | c_t^{(i)}) / \pi_{\text{roll}}(y_t^{(i)} | c_t^{(i)})$ for all t
- 7: Compute position weights: $w_t \leftarrow \min(1, \sqrt{(T_i-t)\delta/2})$
- 8: Compute $W_i \leftarrow \sum_{t=1}^{T_i} |\rho_t^{(i)} - 1| \cdot w_t$
- 9: Normalize: $\tilde{W}_i \leftarrow W_i / Z(T_i)$
- 10: Compute mask: $M_i \leftarrow \mathbb{I}[\tilde{W}_i \leq \delta_W]$
- 11: **end for**
- 12: **Backward Pass:** $\nabla L \leftarrow \frac{1}{N} \sum_{i=1}^N M_i \cdot A^{(i)} \cdot \sum_t \rho_t^{(i)} \nabla \log \pi_\theta(y_t^{(i)} | c_t^{(i)})$
- 13: **Update:** $\theta \leftarrow \theta + \alpha \cdot \nabla L$

2. **Approximation error bound:** If additionally $D_{\text{KL}}^{\text{tok},\text{max}} \leq \delta$ holds globally, the approximation error satisfies:

$$|\text{Error}| \leq 2 \mathbb{E}_{\pi_{\text{roll}}}[W(y)]. \quad (79)$$

In particular, when all trajectories in the support of π_{roll} are accepted (i.e., $\tilde{W}(y) \leq \delta_W$ almost surely), this gives $|\text{Error}| \leq 2 \delta_W \cdot Z(T)$.

Proof. **Part 1** follows directly from the masking criterion: $\tilde{W}_i \leq \delta_W$ implies $W(y^{(i)}) = \tilde{W}_i \cdot Z(T_i) \leq \delta_W \cdot Z(T_i)$.

Part 2. From the tower-property factorization in the proof of Theorem 4.6 (Appendix C, Eq. (69)), when $D_{\text{KL}}^{\text{tok},\text{max}} \leq \delta$:

$$|\text{Error}| \leq 2 \sum_{t=1}^T \mathbb{E}_{\pi_{\text{roll}}} [|\rho_t - 1|] \cdot \min \left(1, \sqrt{\frac{(T-t)\delta}{2}} \right). \quad (80)$$

Since the position weights $\min(1, \sqrt{(T-t)\delta/2})$ are deterministic constants, linearity of expectation gives:

$$|\text{Error}| \leq 2 \mathbb{E}_{\pi_{\text{roll}}} \left[\sum_{t=1}^T |\rho_t - 1| \cdot \min \left(1, \sqrt{\frac{(T-t)\delta}{2}} \right) \right] = 2 \mathbb{E}_{\pi_{\text{roll}}}[W(y)]. \quad (81)$$

If $W(y) \leq \delta_W \cdot Z(T)$ holds for all y in the support, then $\mathbb{E}[W(y)] \leq \delta_W \cdot Z(T)$. \square

Remark D.4. In practice, LN-TRM enforces $W(y) \leq \delta_W \cdot Z(T)$ only for accepted trajectories, not universally. The per-trajectory score $W(y)$ thus serves as an observable diagnostic: a high acceptance rate indicates that $\mathbb{E}[W(y)] \approx \mathbb{E}[W(y) \cdot M] \leq \delta_W \cdot Z(T)$, providing approximate control of the error via Eq. (79).

The bound is $O(\delta_W \cdot Z(T))$. Since $Z(T)$ scales between $O(T)$ (when the min saturates at 1 for most positions) and $O(T^{3/2}\sqrt{\delta})$ (in the Pinsker regime), and the surrogate L also scales as $O(T)$, the monotonic improvement condition is approximately length-neutral.

D.5 Simplified Variant: Sequence-Error Ratio (SER)

For practitioners seeking the minimal change to an existing GRPO or PPO codebase, we propose the Sequence-Error Ratio (SER) algorithm. SER uses an unweighted, length-normalized error score:

$$W_{\text{SER}}(y) := \frac{1}{T} \sum_{t=1}^T |\rho_t - 1|. \quad (82)$$

The masking criterion is $M(y) = \mathbb{I}[W_{\text{SER}}(y) \leq \delta_{\text{SER}}]$ with a fixed, length-independent threshold δ_{SER} .

Algorithm 3 Sequence-Error Ratio (SER)

Require: Threshold δ_{SER} (e.g., 0.05); Batch \mathcal{D}

- 1: **for** each sequence i with length T_i **do**
- 2: Compute $\rho_t^{(i)}$ for all t
- 3: $W_i \leftarrow \frac{1}{T_i} \sum_{t=1}^{T_i} |\rho_t^{(i)} - 1|$
- 4: $M_i \leftarrow \mathbb{I}[W_i \leq \delta_{\text{SER}}]$
- 5: **end for**
- 6: Compute ∇L_{masked} with mask M , normalize by N

Theoretical motivation. SER is connected to the linear bound via the Adaptive bound with the min set to 1. Since $\mathbb{E}_{y_t \sim \mu}[|\rho_t - 1|] = 2D_{\text{TV}}^{\text{tok}}(c_t)$, the score W_{SER} estimates twice the average per-token TV divergence. The linear bound gives $|\text{Error}| \leq 4 \sum_t \bar{D}_t$, so controlling $\sum |\rho_t - 1|/T$ at level δ bounds the per-trajectory error contribution at rate $O(T\delta)$, which scales linearly with T —matching the surrogate’s scaling.

Length neutrality. Because W_{SER} is an average (not a sum), the same threshold δ_{SER} applies uniformly regardless of T . If per-token divergence is i.i.d., the expected score is constant across lengths. The remaining source of length bias is the *variance* of the average, which decreases as $O(1/\sqrt{T})$ by the CLT. This means SER is actually *mildly biased in favor of* longer sequences (their average is more concentrated), which partially counteracts the per-token violation probability effect discussed in Appendix D.1.

Practical recommendation. SER requires adding only three lines of code to any GRPO/PPO implementation:

```

W = mean(abs(rho - 1), dim=-1)  # per-sequence average
M = (W <= delta_ser).float()    # binary mask
loss = loss * M                  # mask rejected sequences

```

We recommend $\delta_{\text{SER}} \in [0.03, 0.10]$ as a starting range, with the masking rate monitored to maintain $\leq 30\%$ rejection.

D.6 Comparison of Length Bias Properties

There is a fundamental tension in trust region methods for sequence generation: the trade-off between the tightness of the theoretical error bound and the practical stability of the training process across varying sequence lengths. Table 3 provides a comparative summary of how different masking criteria behave as the sequence length T increases.

LN-TRM stands out as the theoretically principled choice, as it re-weights the importance ratios according to their influence on the future trajectory, ensuring that early-token deviations—which are more catastrophic for the approximation—are more strictly constrained. Additionally, SER offers

the most practical path for implementation. Its variance actually decreases for longer sequences, meaning the masking becomes more reliable as T grows. This property acts as a helpful counterweight to the inherent difficulty of maintaining low divergence over long horizons, making it an ideal default for large-scale RL training of LLMs.

Table 3: Length bias properties of sequence-level masking methods. “Rejection scaling” describes how the rejection probability grows with T when per-token divergence is constant.

Method	Criterion	Rejection scaling	Formal guarantee
TRM-Max	$\max_t D_{\text{KL}}(c_t) \leq \delta$	$1 - (1 - p)^T$ (exponential)	Exact
TRM-Avg	$\frac{1}{T} \sum_t D_{\text{KL}}(c_t) \leq \delta$	\approx constant	Weaker ($\text{avg} \neq \text{max}$)
LN-TRM	$W(y) \leq \delta_W$	\approx constant	Up to $Z(T)$ factor
SER	$\frac{1}{T} \sum \rho_t - 1 \leq \delta$	\approx constant	Via linear bound